ELSEVIER

ADVANCES IN
COLLOID AND
INTERFACE
SCIENCE

Advances in Colloid and Interface Science
85 (2000) 61–97

www.elsevier.nl/locate/cis

# Which surfactants reduce surface tension faster? A scaling argument for diffusion-controlled adsorption

James K. Ferri, Kathleen J. Stebe*

*Johns Hopkins University, Department of Chemical Engineering, Baltimore, MD 21218, USA*

---

## Abstract

Consider the example of surfactant adsorbing from an infinite solution to a freshly formed planar interface. There is an implicit length scale in this problem, the adsorption depth $h$, which is the depth depleted to supply the interface with the adsorbed surfactant. From a mass balance, $h$ can be shown to be the ratio of the equilibrium surface concentration $\Gamma_{\mathrm{eq}}$ to the bulk concentration $C_\infty$. The characteristic time scale for diffusion to the interface is $\tau_D = h^2/D$, where $D$ is the diffusivity of the surfactant in solution. The significance of this time scale is demonstrated by numerically integrating the equations governing diffusion-controlled adsorption to a planar interface. The surface tension equilibrates within 1–10 times $\tau_D$ regardless of bulk concentration, even for surfactants with strong interactions. Dynamic surface tension data obtained by pendant bubble method are rescaled using $\tau_D$ to scale time. For high enough bulk concentrations, the re-normalized surface tension evolutions nearly superpose, demonstrating that $\tau_D$ is indeed the relevant time scale for this process. Surface tension evolutions for a variety of surfactants are compared. Those with the smallest values for $\tau_D$ equilibrate fastest. Since diffusion coefficients vary only weakly for surfactants of similar size, the differences in the equilibration times for various surfactant solutions can be attributed to their differing adsorption depths. These depths are determined by the equilibrium adsorption isotherms, allowing $\tau_D$ to be calculated a priori from equilibrium surface tension data, and surfactant solutions to be sorted in terms of which will reduce the surface tension more rapidly. Finally, trends

---

* Corresponding author. Tel.: +1-410-516-7769; fax: +1-410-516-5510.
*E-mail address:* kjs@jhu.edu (K.J. Stebe)

PII: S0001-8686(99)00027-5

predicted by $\tau_D$ to gauge what surfactant properties are required for rapid surface tension reduction are discussed. These trends are shown to be in agreement with guiding principles that have been suggested from prior structure–property studies.

*Keywords:* Surfactant mass transfer; Adsorption; Dynamic surface tension; Structure–property studies of surfactants; Surfactant interactions

---

## Contents

## 1. Introduction: $\tau_D$, a diffusion time scale

Surfactants are added to reduce the surface tension in a variety of processes where interface is created [1,2], e.g. in the creation of coatings or sprays, and in the mixing of fluids to create foams or emulsions. Such processes occur frequently in the petroleum industry [3], in the application of agricultural chemicals [4], and in the foods [5], cosmetics [6], paper and textiles industries [7,8]. Since the formation of the interface is a dynamic process, the effectiveness of surfactant additives is influenced by the rate of delivery of surfactant to the interface as well as the thermodynamics which determine how a given surfactant reduces the equilibrium surface tension. The equilibrium surface tension $\gamma_{eq}$ depends on the tendency of the surfactant to adsorb, and the sensitivity of the surface tension to the adsorbed surfactant. The simplest model which adequately describes the gross equilibrium behavior of a wide variety of surfactants [9] is the Langmuir isotherm:

$$\frac{\Gamma_{\mathrm{eq}}}{\Gamma_\infty} = \frac{C_\infty/a}{1 + C_\infty/a} \tag{1}$$

and the Von Szyckowski surface equation of state.

$$\gamma_{\mathrm{eq}} = \gamma_o + RT\Gamma_\infty \ln\left(1 - \frac{\Gamma_{\mathrm{eq}}}{\Gamma_\infty}\right) = \gamma_o - RT\Gamma_\infty \ln(1 + C_\infty/a) \tag{2}$$

where $RT$ is the product of the ideal gas constant and the temperature. This two-parameter model assumes monolayer adsorption; $a$ gives the tendency to adsorb at the interface and $\Gamma_\infty$ is the maximum packing on the interface, which can be related to the size of the adsorbed surfactant (i.e. $\Gamma_\infty$ is often interpreted as the inverse minimum area/molecule).

These same isotherm parameters can lend insight into the rate of surface tension reduction. Consider a surfactant solution immediately after the interface is formed. Surfactant adsorbs, depleting the local concentration. This causes surfactant to diffuse from the bulk solution to supply this region. Therefore, both the kinetics of surfactant adsorption–desorption and the bulk diffusion determine the rate of surfactant adsorption. Often, bulk diffusion is the controlling mechanism (see the reviews by Chang and Franses [9] and Miller et al. [10]). The characteristic time scale for diffusion depends upon how effectively the interface depletes the solution, and the diffusivity, $D$, of the surfactant molecule. Most surfactants have $D \approx 5 \times 10^{-6}$ cm$^2$/s; yet they differ strongly in the rate at which they reduce the surface tension. The differences arise from the adsorption depth, $h$, which is the depth depleted by surfactant adsorption. This depth can be used to define the diffusion time scale:

$$\tau_D = \frac{h^2}{D} \tag{3}$$

At elevated concentrations the interface becomes ineffective at diluting the solution, causing $h$ (and therefore $\tau_D$) to decrease.

The adsorption depth $h$ can be derived from a mass balance on a differential area $\mathrm{d}A$. The adsorbed mass of surfactant is given by $\Gamma_{\mathrm{eq}}\mathrm{d}A$. In the fluid beneath the interface, the same amount of mass would be found in a volume $h\mathrm{d}A$; the mass of surfactant in that volume is given by $C_\infty h\mathrm{d}A$. Equating the two expressions for the mass and solving for $h$ yields:

$$h = \frac{\Gamma_{\mathrm{eq}}}{C_\infty} \tag{4}$$

which, for a Langmuir model is:

$$h = \frac{\Gamma_{\text{eq}}}{C_\infty} = \frac{\Gamma_\infty / a}{1 + C_\infty / a} \tag{5}$$

Together, Eqs. (3) and (5) allow the prediction of the time scales for diffusion-controlled surface tension relaxation for a given surfactant from its equilibrium parameters and its diffusivity. [If the surfactant is described in terms of a more complex isotherm, the same argument can be used to define $h$ according to Eq. (4) and the relevant isotherm parameters. This is discussed in the context of the Frumkin [11] isotherm for surfactants with repulsive or attractive interactions, or the Davies isotherm [12] for ionic surfactants.]

Because $\tau_D$ is the characteristic time scale for surface tension relaxation, it provides a basis for comparing surfactants in order to predict which is more effective at rapidly reducing the surface tension.

Dynamic surface tension studies are performed by creating interface in some controlled manner, and measuring the change in surface tension as a function of time. The techniques to perform these measurements can be hydrostatic (e.g. the pendant bubble technique or the Wilhelmy plate technique), or, they can have leading order flow (e.g. the maximum bubble pressure technique; the drop weight method; the oscillating jet method, etc.). The implications of $\tau_D$ are discussed below first for the hydrostatic methods. The utility of these arguments in systems with convection is discussed in Section 4.

## 2. Diffusion-controlled adsorption

### 2.1. Predicted surface tension relaxations of non-interacting surfactants

At $t = 0$, an interface is exposed to a quiescent surfactant solution. The surface concentration and sublayer concentration are initially zero:

$$\Gamma(t = 0) = 0; \quad C_s(t = 0) = C(z = 0,\ t = 0) = 0 \tag{6}$$

Surfactant partitions between the sublayer and the interface according to the adsorption isotherm [Eq. (1)]. The diffusion-controlled evolution in the surface concentration $\Gamma(t)$ is given by the Ward and Tordai [13] equation:

$$\Gamma(t) = \frac{2\sqrt{D}}{\sqrt{\pi}} \left[ C_\infty \sqrt{t} - \int_0^{\sqrt{t}} C_s(t - \tau) \mathrm{d}\sqrt{\tau} \right] \tag{7}$$

The simultaneous solution of Eqs. (1) and (7) subject to the initial condition [Eq. (6)] defines the evolution of the surface concentration $\Gamma(t)$ [14]. Evaluating Eq. (2) for each time step, the surface tension evolution $\gamma[\Gamma(t)]$ is determined. For a given surfactant, then, if the isotherm parameters and the diffusion coefficient are known, the surface tension relaxation can be predicted. The isotherm parameters are found by fitting Eq. (2) to equilibrium surface tension data as a function of bulk concentration. Diffusion coefficients can be obtained either by independent means or by fitting dynamic surface tension traces. Lin et al. [15] performed such a study for Triton-X 100. Using the parameters that they found for Triton-X 100, the predicted evolution of the surface concentration and the surface tension, respectively, are shown in Fig. 1a,b as a function of bulk concentration. Similar surface tension profiles (amended only in that mass transfer to a sphere rather than a plane was modeled) were shown to agree favorably with pendant bubble data in that study. Both the equilibrium adsorption and the adsorption rate increase with concentration. In order to focus on the rate, these equations are re-scaled:

$$C' = \frac{C}{C_\infty}; \quad \Gamma' = \frac{\Gamma}{\Gamma_{\text{eq}}}; \quad t' = \frac{t}{\tau_D}; \quad \theta = \frac{\gamma(t) - \gamma_{\text{eq}}}{\gamma_o - \gamma_{\text{eq}}} \tag{8}$$

Initially the surface tension is given by the clean interface value, so $\theta = 1.0$. When the surface tension attains equilibrium, $\theta = 0$. In terms of these dimensionless variables,

$$\Gamma'(t') = 2\sqrt{\frac{1}{\pi}}\left[\sqrt{t'} - \int_0^{\sqrt{t'}} C_s'(t' - \tau)\mathrm{d}\sqrt{\tau}\right] \tag{9}$$

$$x\Gamma'(t') = \frac{kC_s'(t')}{1 + kC_s'(t')} \tag{10}$$

$$\theta = 1 - \frac{\ln[1 - x\Gamma'(t')]}{\ln(1 - x)} \tag{11}$$

In these expressions, two dimensionless parameters appear. The adsorption number $k$, a scaled bulk concentration:

$$k = \frac{C_\infty}{a} \tag{12}$$

and the equilibrium surface coverage, $x$:

$$x = \frac{\Gamma_{\text{eq}}}{\Gamma_\infty} \tag{13}$$

For Langmuir, $x = k/(1 + k)$. The scaled concentration $k$ appears explicitly in these equations, and is therefore not isolated in the time scale $\tau_D$. Consequently, even in this re-scaled form, the surface tension reduction will vary with $k$. The dimensionless graphs of $\Gamma'(t')$ and $\theta(t')$, respectively, are presented in Fig. 2a,b as

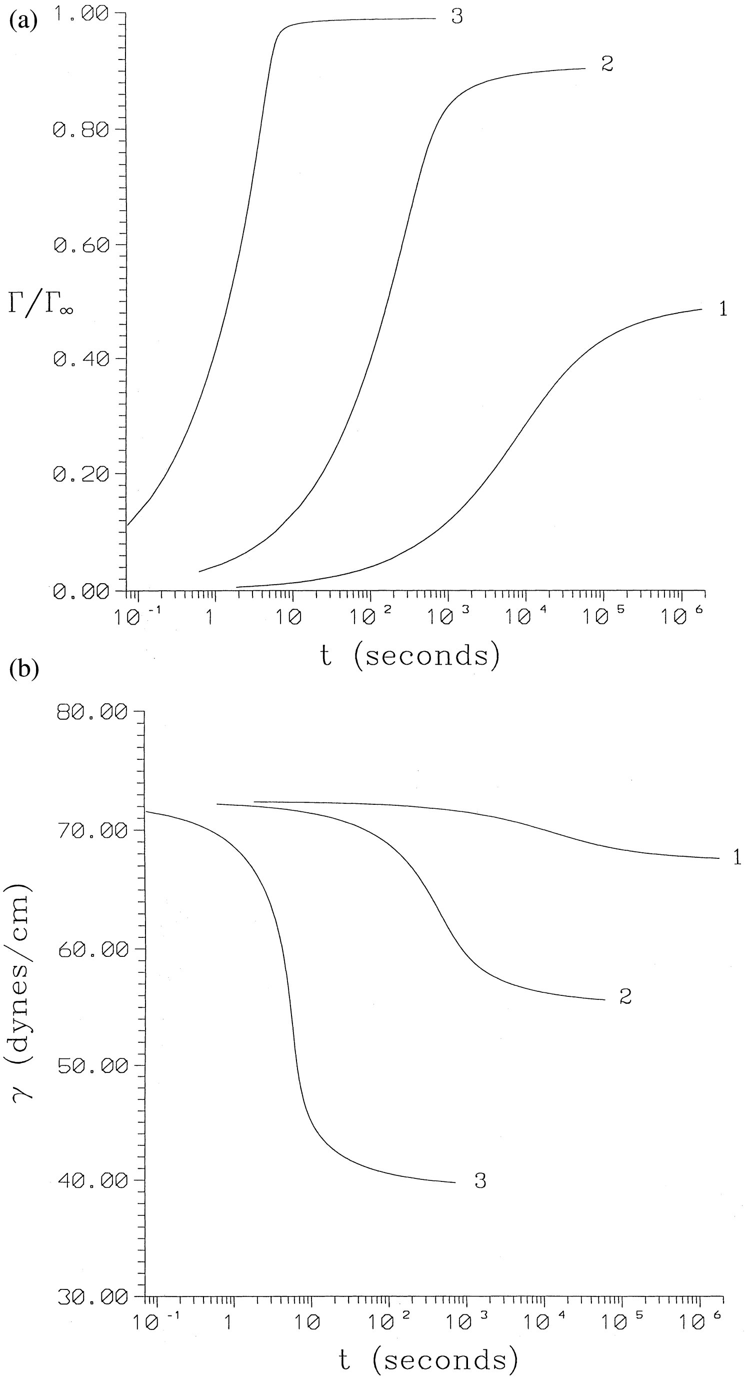

Fig. 1. The predicted evolution for Triton-X 100 of (a) the surface concentration $\Gamma$ and (b) the surface tension $\gamma$, respectively, as a function of bulk concentration $C_\infty$ in mol/cm$^3$: (1) $C_\infty = 6.6 \times 10^{-10}$, $k = 1.0$; (2) $C_\infty = 6.6 \times 10^{-9}$, $k = 10.0$; and (3) $C_\infty = 6.6 \times 10^{-8}$, $k = 100$; using the Langmuir parameters and diffusion coefficient in Table 1.

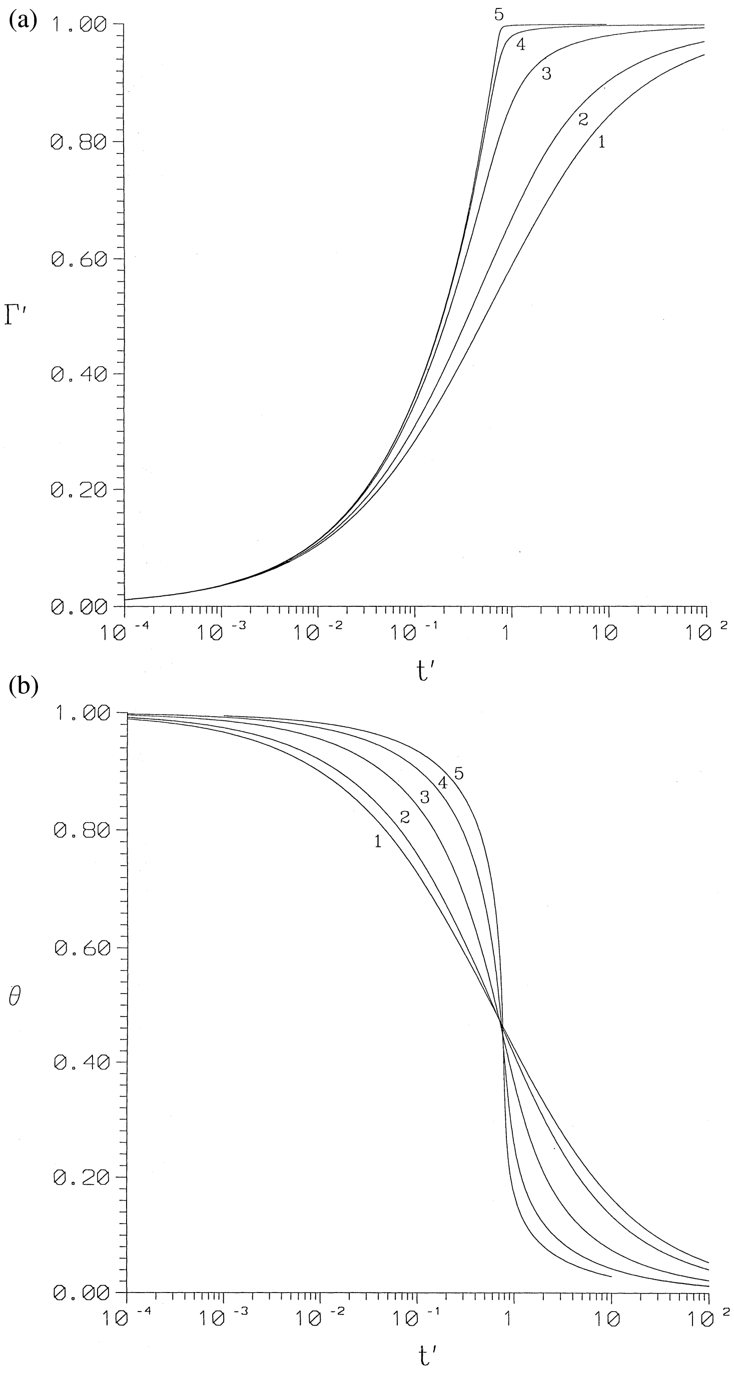

Fig. 2. The dimensionless graphs of (a) $\Gamma(t')$ and (b) $\theta(t')$ for any surfactant which obeys the Langmuir adsorption isotherm as a function of adsorption number $k$: (1) $k = 0.1$; (2) $k = 1.0$; (3) $k = 10$; (4) $k = 100$; and (5) $k = 1000$.

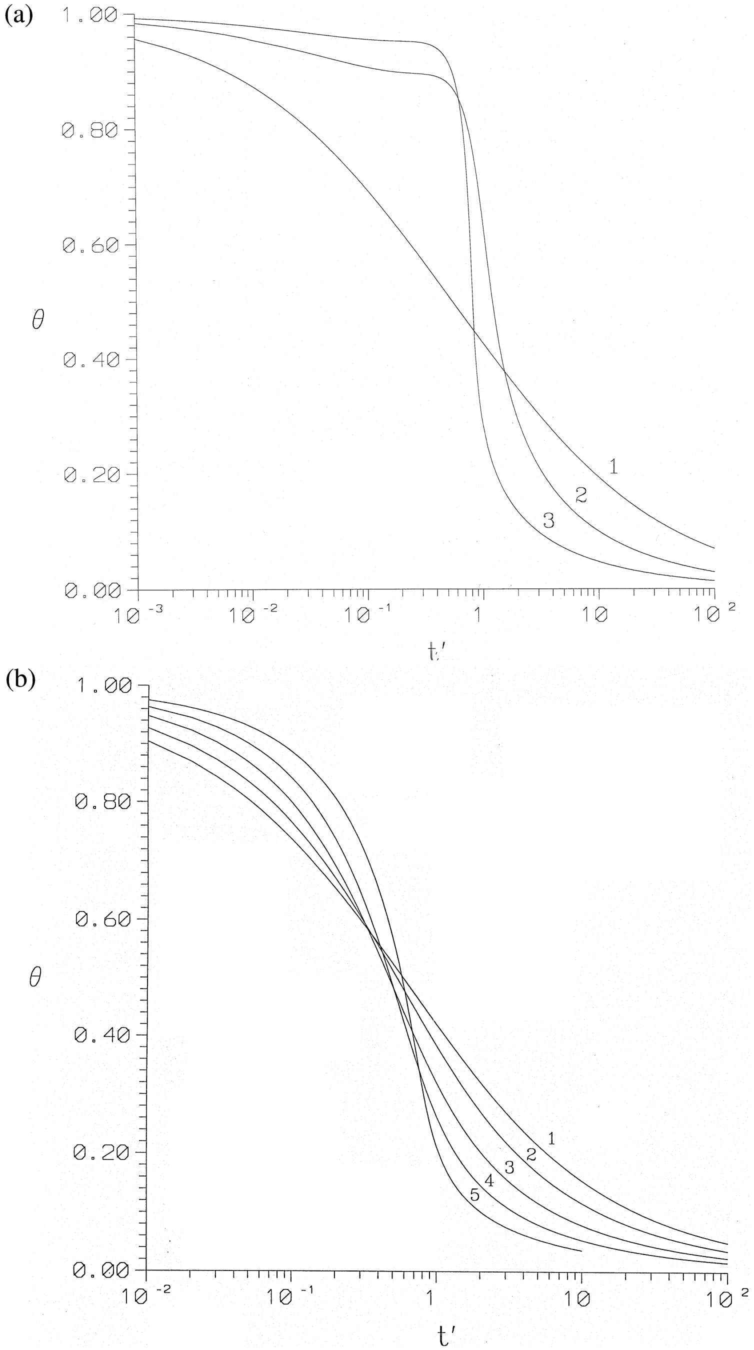

Fig. 3. The evolution of $\theta(t')$ for (a) fixed attractive interactions ($K = -3.9$) and (b) fixed repulsive interactions ($K = 3.0$), as a function of adsorption number $k$: (1) $k = 0.1$; (2) $k = 1.0$; (3) $k = 10$; (4) $k = 100$; and (5) $k = 1000$.

a function of $k$. These curves represent the solution to the surface tension evolution for diffusion-controlled adsorption for *all* surfactants obeying the Langmuir adsorption isotherm. The greater is $k$, the faster is the reduction in $\theta$ for $0.5 < \theta < 0$. For $k \gg 1$, this dependence is fairly weak.

For all of the curves in Fig. 2b, the system has attained 50% of its final surface tension reduction when the dimensionless time $t'$ is unity, and between 80 and 90% of its equilibrium when $t' = 10$. That is, within $10\tau_D$, the system has nearly attained equilibrium for any surfactant obeying the Langmuir framework.

### 2.2. Predicted surface tension relaxations of interacting surfactants

The Langmuir isotherm neglects interactions among the adsorbed surfactants. There have been several recent studies which underscore the importance of attractive or repulsive interactions among surfactants in the dynamic surface tension [16–25]. Here, the simplest model which incorporates these effects, the Frumkin isotherm, is adopted to illustrate the importance of $\tau_D$ for a diffusion controlled surfactant with pronounced interactions. For the Frumkin model, Eqs. (10) and (11) are replaced with:

$$x\Gamma'(t') = \frac{kC_s(t')}{\exp[Kx\Gamma'(t')] + kC_s(t')} \tag{14}$$

$$\theta = 1 - \frac{\ln[1 - x\Gamma'(t')] - K[x\Gamma'(t')]^2/2}{\ln(1 - x) - Kx^2/2} \tag{15}$$

where $k$ and $x$ are defined in Eqs. (12) and (13). The parameter $K$ accounts for nearest neighbor interactions among adsorbed surfactants; for attractive interactions, $K < 0$; for repulsive interactions, $K > 0$. Eqs. (9), (14) and (15) are solved simultaneously to find $\theta(t')$ for fixed attractive ($K = -3.9$) or repulsive ($K = 3.0$) interactions; the results are presented in Fig. 3a,b, respectively. For attractive interactions, a shoulder develops in the dynamic surface tension profile for large enough $k$. For $k \gg 1$, $\theta$ depends only weakly on $k$; the surface tension drops strongly at $t' \approx 1.0$ (i.e. when $\tau_D$ seconds have passed). For repulsive interactions, $\theta(t')$ is qualitatively similar to the Langmuir case, except that equilibrium is attained at slightly earlier times. Thus, regardless of whether surfactants attract or repel each other at the interface, within 1–10 $\tau_D$, the surface tension approaches its equilibrium value provided the scaled concentration $k \gg 1$.

When a charged surfactant adsorbs, it creates a repulsive electrical potential at the interface $\Psi_s$ which alters the adsorption of the surfactant and the surface tension response. For equivalent species, the Davies adsorption isotherm [12]:

$$x\Gamma'(t') = \frac{kC_s(t')}{\exp[(-zF\Psi_s)/(RT)] + kC_s(t')} \tag{16a}$$

and the Gouy–Chapman model for the surface potential:

$$\frac{\Gamma(t)}{\Sigma C_{i\infty}} = \frac{1}{\kappa}\left\{\frac{C_s(t) + C_{3\infty}}{\Sigma C_{i\infty}}\right\}^{1/2} \sinh\left(\frac{|z|\, F\Psi_s}{2RT}\right) \tag{16b}$$

where

$$\kappa^{-1} = \sqrt{\frac{\epsilon RT}{F^2 \sum_{i=1}^{4} C_{i\infty}}} \tag{16c}$$

have been proposed to describe the partitioning of surfactant between the bulk and interface in a solution of equivalent surfactant and salts. In these expressions, $\kappa$ is the inverse Debye length, $z$ is the valence of the ionic species, and $F$ is Faraday's constant. $C_s$ is the instantaneous surfactant sublayer concentration, $C_{3\infty}$ is the bulk concentration of the co-ion of the added salts, and the summation in the denominator of Eq. (16b) is over the bulk concentrations of all ionic species in solution. The corresponding model for the surface tension is [12]:

$$\begin{aligned}\gamma(t) = \gamma_o + RT\Gamma_\infty \ln\left(1 - \frac{\Gamma(t)}{\Gamma_\infty}\right) + \frac{4RT}{zF}[2\epsilon RT(C_s(t) + C_{3\infty})]^{1/2} \\ \times\left[1 - \cosh\left(\frac{zF\Psi_s(t)}{2RT}\right)\right]\end{aligned} \tag{17a}$$

which can be recast in terms of $\theta(t')$

$$\begin{aligned}\theta(t') = 1 - \frac{\ln(1 - \Gamma'(t'))}{\ln(1 - \Gamma'_{\text{eq}}) + \dfrac{4}{(z_1\kappa h)}\left[1 - \cosh\left(\dfrac{z_1\Psi'_{\text{eq}}}{2}\right)\right]} \\ - \frac{\dfrac{4}{(z_1\kappa h)}\left[\sqrt{2\left(C'_{1s}(t')\hat{C}_{1\infty} + \hat{C}_{3\infty}\right)}\right]\left[1 - \cosh\left(\dfrac{z_1\Psi'_s(t')}{2}\right)\right]}{\ln(1 - \Gamma'_{\text{eq}}) + \dfrac{4}{(z_1\kappa h)}\left[1 - \cosh\left(\dfrac{z_1\Psi'_{\text{eq}}}{2}\right)\right]}\end{aligned} \tag{17b}$$

This is the quasi-equilibrium model posed by Macleod and Radke [26]. Eqs. (9), (16a), (16b), (16c) and (17b) were integrated by Datwani and Stebe [27] for the constants reported by Fainerman [28] for SDS. The results are presented in Fig. 4. In this graph, time is scaled with $\tau_D$ as defined in Eq. (3) where $h$ is found using the Davies isotherm fit to SDS. The ionic strength in these simulations was weak, corresponding to 0.05 M NaCl. Once again, all of the model traces reach equilibrium on times comparable to $\tau_D$.

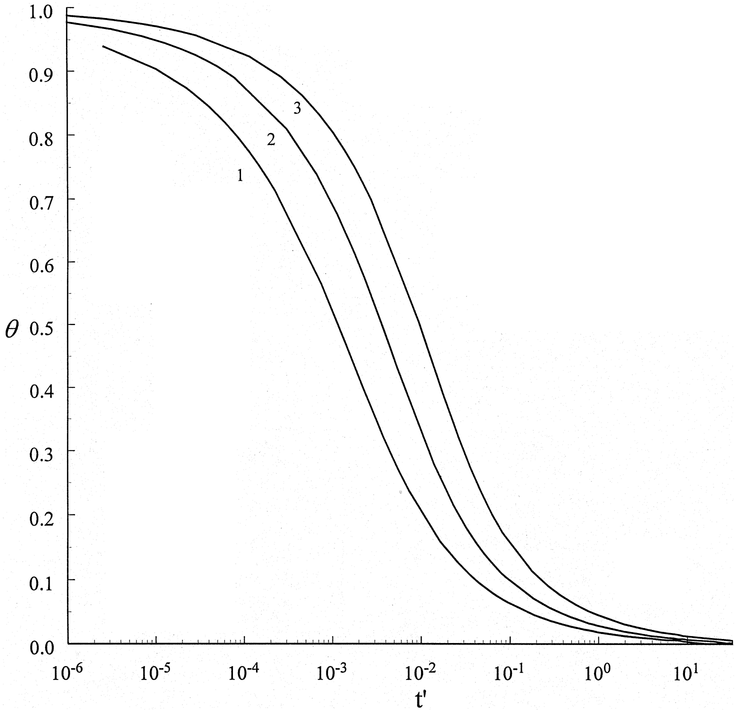

Fig. 4. The evolution of $\theta(t')$ for the adsorption of a charged surfactant for diffusion-controlled adsorption for a monovalent surfactant: (1) $k = 1$; (2) $k = 10$; and (3) $k = 100$.

## 3. Normalizing dynamic surface tension data with $\tau_D$

The equilibrium surface tension, isotherm and the surface tension evolution at the air–aqueous interface have been reported and analyzed in detail for a number of surfactants using the pendant bubble technique. Below, dynamic surface tension data from the literature are discussed for four different surfactants. Typically, mass transfer to a pendant bubble is modeled as mass transfer to a sphere [15]. The expression for the evolution in the surface concentration driven by diffusion flux to a spherical bubble of radius $a_B$ is:

$$\Gamma'(t') = 2\sqrt{\frac{1}{\pi}}\left[\sqrt{t'} - \int_0^{\sqrt{t'}} C_s'(t' - \tau)\mathrm{d}\sqrt{\tau}\right] + \frac{h}{a_B}\left[t' - \int_0^{t'} C_s(\tau)\mathrm{d}\tau\right] \tag{18}$$

in dimensionless form. The diffusion flux to a spherical bubble of radius $a_B$ has two terms associated with curvature of the interface; these terms have a characteristic time scale associated with them of $\tau_D h / a_B$; that is, curvature alters the mass transfer when the adsorption depth is large compared to the bubble radius.

Table 1
Equilibrium constants, diffusion coefficient, and critical micelle concentration[a]

| | $\Gamma_\infty \times 10^{10}$ | $a \times 10^9$ | $K$ | $D \times 10^6$ | CMC $\times 10^{7}$[b] |
|---|---|---|---|---|---|
| $C_{10}E_8$ [29] | | | | | |
| (L) | 1.80 | 0.544 | 0 | 4.3 | 12 |
| (F) | 3.07 | 0.130 | 9.6 | | |
| $C_{12}E_8$ [30] | | | | | |
| (L) | 2.04 | 0.0768 | 0 | 4.8 | 1.0 |
| (F) | 2.67 | 0.0250 | 5.2 | | |
| $C_{12}E_6$ [20] | | | | | |
| (L) | 2.42 | 0.114 | 0 | 3.5 | 0.90 |
| (F) | 3.48 | 0.0349 | 6.7 | | |
| TRX-100 [15] | | | | | |
| (L) | 2.91 | 0.662 | 0 | 2.6 | 2.3 |
| (F) | 3.20 | 0.311 | 2.5 | | |
| Surfynol 104 [31] | | | | | |
| (L) | 2.42 | 5.03 | 0 | 4.8[c] | 25 |
| 2,7-Dimethyl-4-octyn-3,6-diol [31] | | | | | |
| (L) | 3.01 | 422 | 0 | 5.4[c] | 240 |
| 7-Tetradecyn-6,9-diol [24] | | | | | |
| (F) | 2.98 | 12.2 | −4.5 | 4.4[c] | 2.2 |
| 1-Decanol [23] | | | | | |
| (F) | 6.17 | 74 | −3.5 | 6.7 | 2.1 |
| 1-Octanol [32] | | | | | |
| (L) | 8.96 | 557 | 0 | 7.3 | 30 |
| (F) | 5.91 | 765 | −2.7 | | |

[a] $\Gamma_\infty$ is reported in mol/cm$^2$; $a$ is reported in mol/cm$^3$; $K$ is dimensionless; $D$ is reported in cm$^2$/s; and CMC is reported in mol/cm$^3$. (L) indicates Langmuir isotherm parameters; and (F) indicates Frumkin isotherm parameters.

[b] For surfactants that do not form micelles, the miscibility limit is reported.

[c] Denotes diffusion coefficient as measured by PFGSE-NMR. All other diffusion coefficients reported are average values of the best fit of the surface tension relaxations.

Typically, $a_B$ is approximately 1 mm. Here, for most of the cases discussed, $h / a_B \leq 1$, so that the effects of curvature are secondary. By re-scaling the raw surface tension data, and presenting it in terms of $\theta$ vs. $t'$, the applicability of the characteristic diffusion time scale $\tau_D$ to these experiments is established.

In Table 1, the isotherm parameters and diffusivities are presented for a number of surfactants for which surface tension relaxation data are available in the literature, along with the critical micelle concentration (or the miscibility limit). These data were drawn from several references [15,20,23,24,29–32].

The scaling argument presented here is not nearly as sensitive to the typically small variation in the diffusion coefficient $D$ from surfactant to surfactant as it is to changes in the adsorption depth $h$. However, whenever possible, diffusion coefficients obtained by independent means have been used. For example, the diffusivities of each of the three diols discussed in this paper were obtained by PFGSE-NMR, a technique reviewed by Stilbs [33]. In the event that data is drawn

(a)

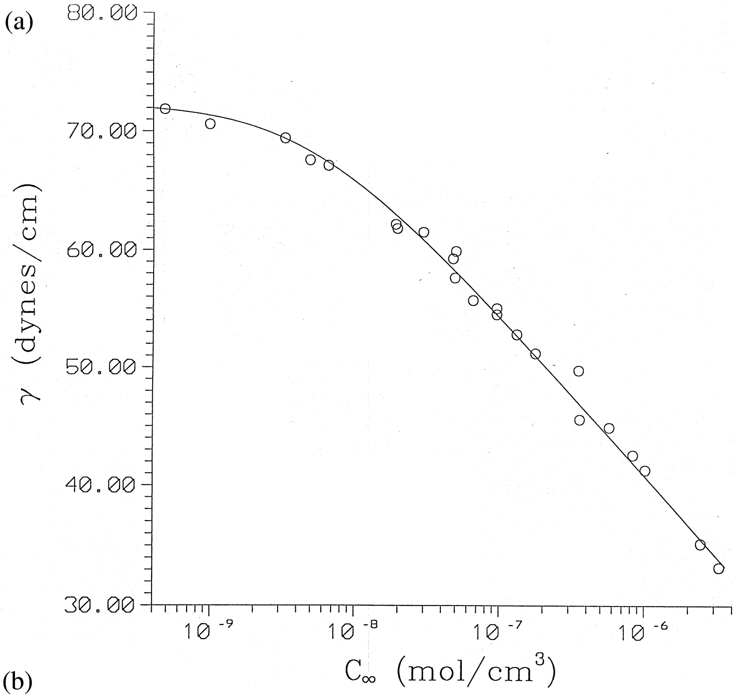
80.00
70.00
60.00
50.00
40.00
30.00
γ (dynes/cm)
10 -9
10 -8
10 -7
10 -6
C∞ (mol/cm3)

(b)

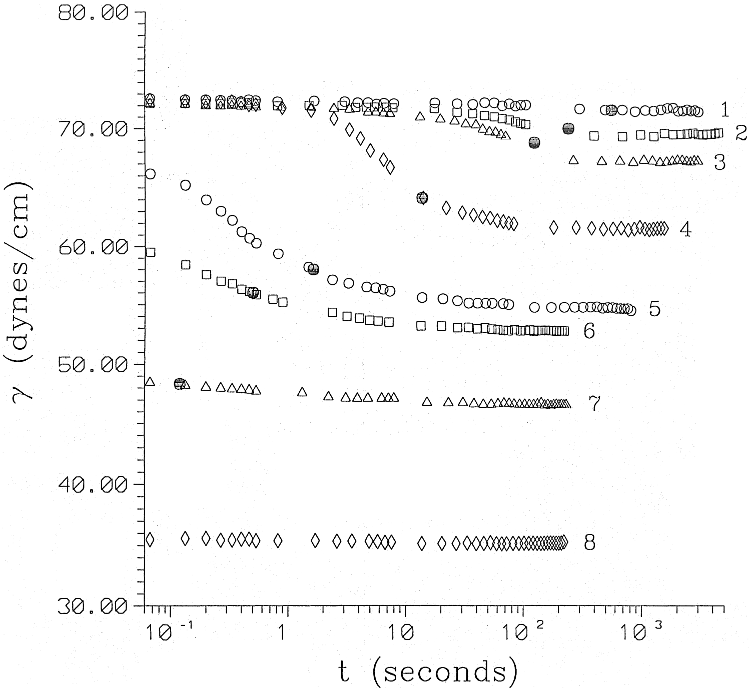
80.00
70.00
60.00
50.00
40.00
30.00
γ (dynes/cm)
10 -1
1
10
10 2
10 3
t (seconds)
1
2
3
4
5
6
7
8

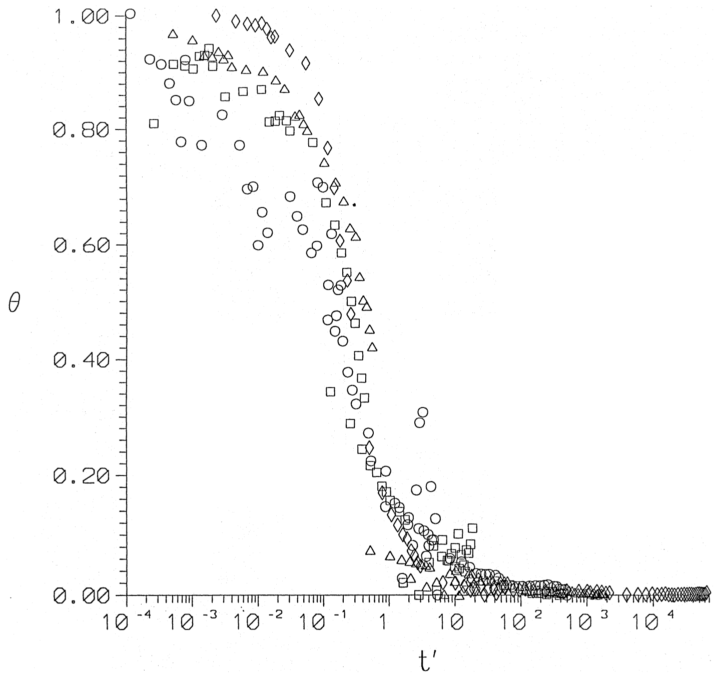

Fig. 5. (a) $\gamma_{eq}$ (dyn/cm) vs. $C_\infty$ for Surfynol 104 with the best-fit Langmuir model shown as the solid curve; the isotherm parameters are given in Table 1. (b) $\gamma$ (dyn/cm) vs. $t$ (s) for Surfynol 104 for $C_\infty$ in mol/cm$^3$: (1) $C_\infty = 4.82 \times 10^{-10}$; (2) $C_\infty = 3.32 \times 10^{-9}$; (3) $C_\infty = 6.64 \times 10^{-9}$; (4) $C_\infty = 3.00 \times 10^{-8}$; (5) $C_\infty = 9.69 \times 10^{-8}$; (6) $C_\infty = 1.33 \times 10^{-7}$; (7) $C_\infty = 3.61 \times 10^{-7}$; and (8) $C_\infty = 2.22 \times 10^{-6}$. (c) The dynamic surface tension of Surfynol 104 in (b) normalized in terms of θ vs. $t'$: (1) $k = 0.0964$, $\tau_D = 406$ s; (2) $k = 0.664$, $\tau_D = 176$ s; (3) $k = 1.32$, $\tau_D = 90$ s; (4) $k = 6.00$, $\tau_D = 10$ s; (5) $k = 19.4$, $\tau_D = 1$ s; (6) $k = 26.6$, $\tau_D = 0.6$ s; (7) $k = 72.2$, $\tau_D = 0.09$ s; and (8) $k = 444$, $\tau_D = 0.002$ s.

from more than one reference for a given surfactant, it is noted in the corresponding figure caption. These constants are used to calculate θ and $\tau_D$. The references from which these isotherm fits and the surface tension data discussed below were drawn are also cited in Table 1.

### 3.1. A surfactant with negligible interactions: Surfynol 104

Surfynol 104 can be adequately described using a Langmuir model. The equilibrium surface tension as a function of bulk concentration is reproduced in Fig. 5a. These data are fitted to Eq. (2) to find the best fit Langmuir parameters. In Fig. 5b, the dynamic surface tension is reproduced for eight concentrations ranging from $4.8 \times 10^{-10}$ to $2.2 \times 10^{-6}$ mol/cm$^3$. The time scale $\tau_D$ was calculated for each concentration using the Langmuir parameters found from the equilibrium study. Using the $\tau_D$ for each concentration to normalize time (i.e. recasting the abscissa as $t' = t/\tau_D$), and recasting the surface tension at each time step in terms of θ, the

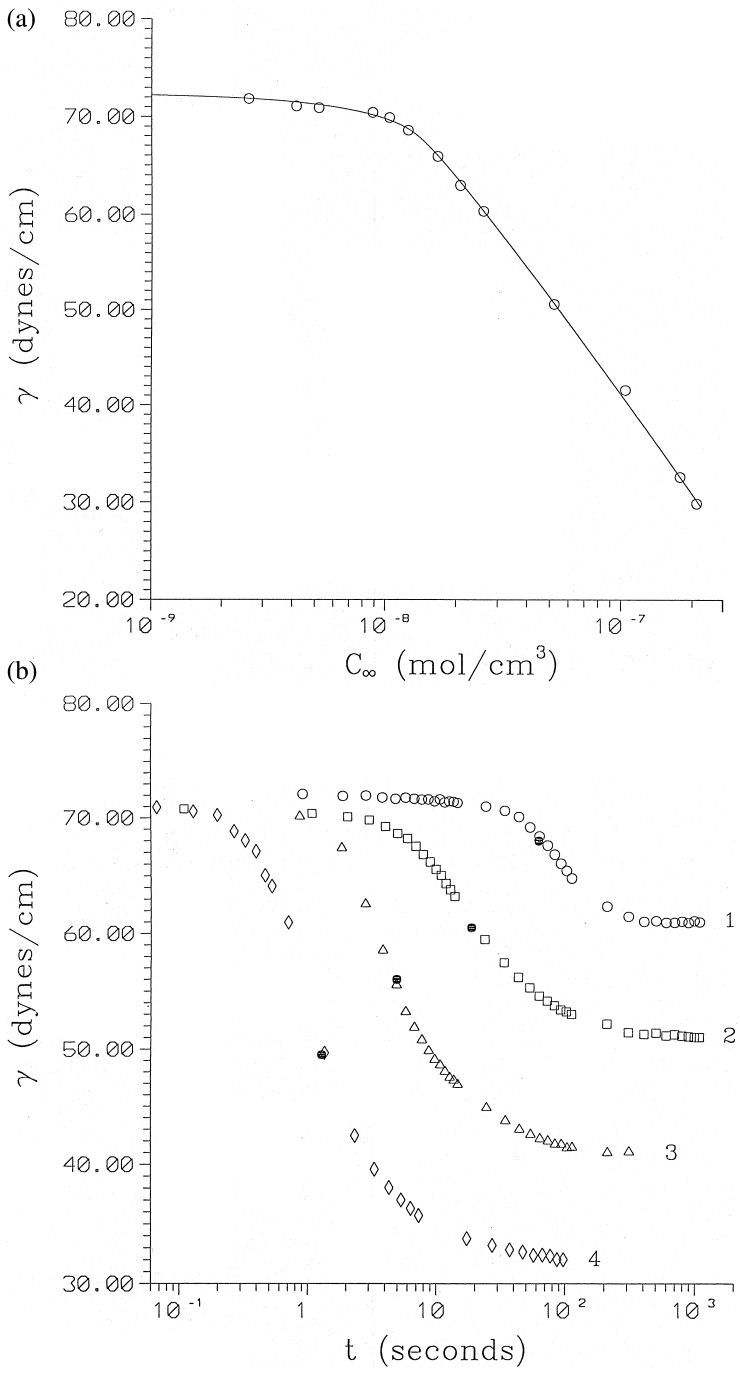
(a)
80.00
70.00
60.00
50.00
40.00
30.00
20.00
γ (dynes/cm)
10 -9
10 -8
10 -7
C∞ (mol/cm3)
(b)
80.00
70.00
60.00
50.00
40.00
30.00
γ (dynes/cm)
10 -1
1
10
10 2
10 3
t (seconds)
1
2
3
4

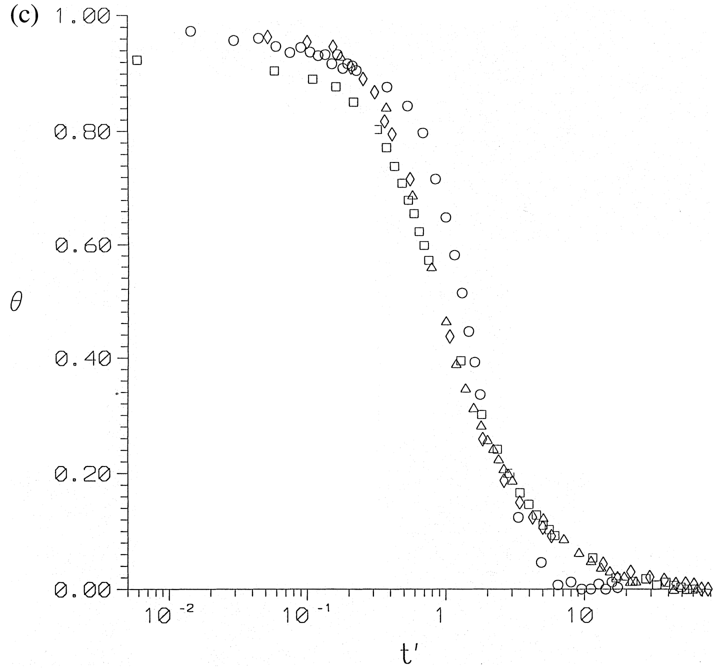

Fig. 6. (a) The equilibrium surface tension vs. bulk concentration for 1-decanol. The solid line is the best fit to the Frumkin equation; the isotherm parameters are in Table 1. (b) $\gamma$ (dyn/cm) vs. $t$ (s) of 1-decanol for $C_\infty$ in mol/cm$^3$: (1) $C_\infty = 2.62 \times 10^{-8}$; (2) $C_\infty = 5.24 \times 10^{-8}$; (3) $C_\infty = 1.05 \times 10^{-7}$; and (4) $C_\infty = 2.09 \times 10^{-7}$. (c) The data in (b) normalized in terms of $\theta$ vs. $t'$: (1) $k = 0.35$, $\tau_D = 64$ s; (2) $k = 18.9$, $\tau_D = 19$ s; (3) $k = 1.42$, $\tau_D = 5$ s; and (4) $k = 2.82$, $\tau_D = 1$ s.

data are presented again in Fig. 5c; the $k$ values corresponding to each concentration are also reported. For most cases, $k \gg 1$; the relaxations in $\theta$ collapse to fall steeply for $t'$ between 1 and 10, i.e. the interface nearly equilibrates within $10\tau_D$ for all cases.

### 3.2. Surfactants with attractive interactions: 1-decanol and 7-tetradecyn-6,9-diol

Both 1-decanol and for 7-tetradcyn-6,9-diol were chosen because they have strong attractive interactions, and require large, negative $K$ values to describe their equilibrium surface tension. The equilibrium surface tension as a function of bulk concentration for 1-decanol is reproduced in Fig. 6a. Dynamic surface tension profiles for concentrations ranging from $2.6 \times 10^{-8}$ to $2.1 \times 10^{-7}$ mol/cm$^3$ are reproduced in Fig. 6b. The time scale $\tau_D$ was calculated at each concentration using the Frumkin parameters determined from fitting the $\gamma_{eq}$ vs. $C_\infty$ data. The raw surface tension data are re-cast in Fig. 6c as a $\theta$ vs. $t'$ plot; these curves again nearly superpose. The surface tension drops strongly for $t'$ between 1 and 10 for all concentrations. The data for 7-tetradecyn-6,9-diol are manipulated in a similar

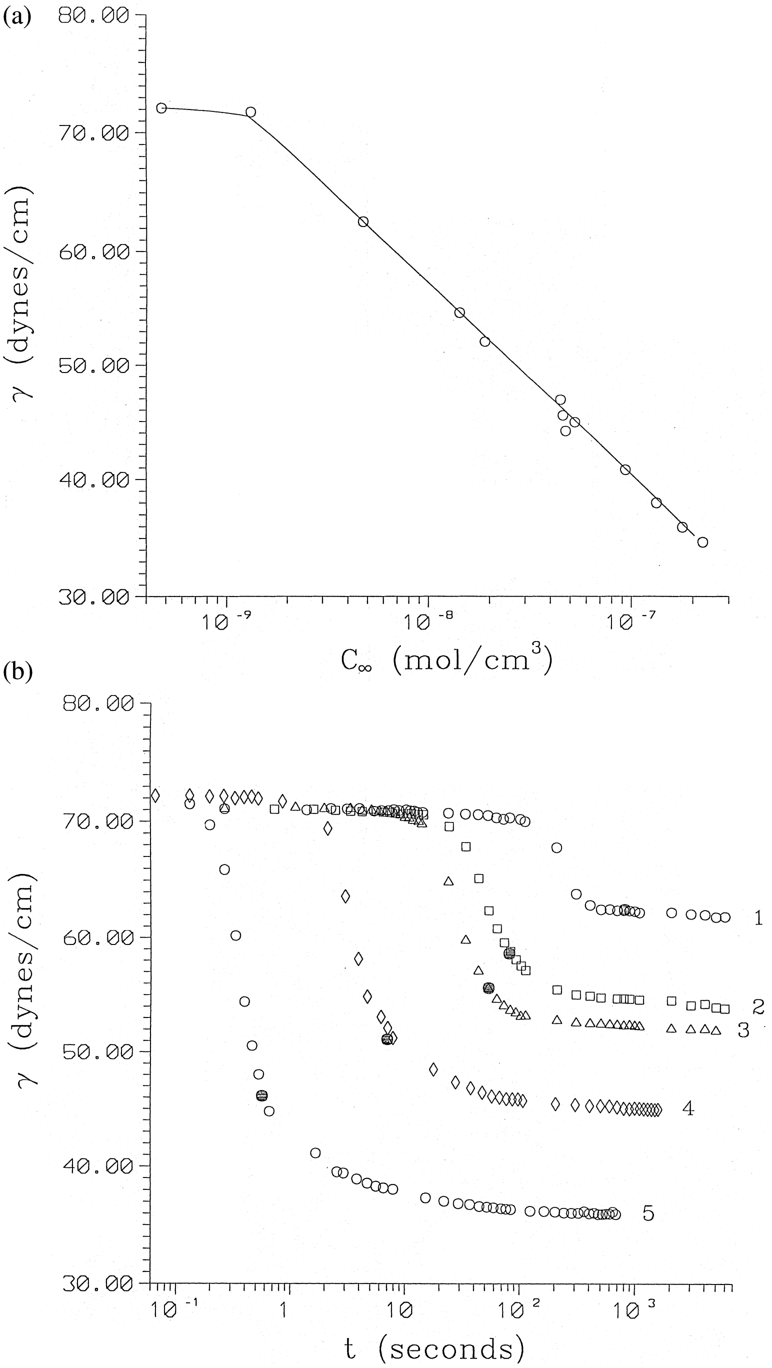
(a)
80.00
70.00
60.00
50.00
40.00
30.00
γ (dynes/cm)
10⁻⁹
10⁻⁸
10⁻⁷
C∞ (mol/cm³)
(b)
80.00
70.00
60.00
50.00
40.00
30.00
γ (dynes/cm)
1
2
3
4
5
10⁻¹
1
10
10²
10³
t (seconds)

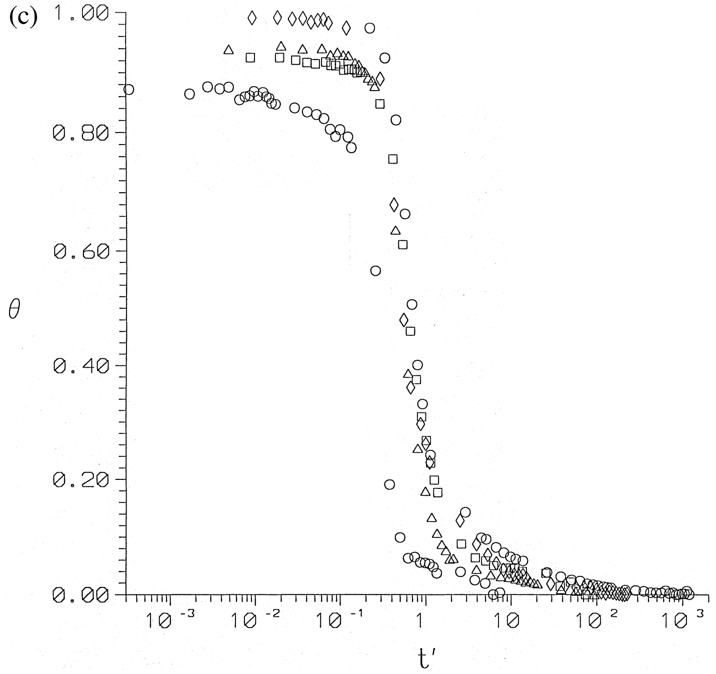

Fig. 7. (a) The equilibrium surface tension vs. bulk concentration for 7-tetradecyn-6,9-diol. The solid line is the best fit to the Frumkin equation; the isotherm parameters are in Table 1. (b) $\gamma$ (dyn/cm) vs. $t$ (s) of 7-tetradecyn-6,9-diol for $C_\infty$ in mol/cm$^3$: (1) $C_\infty = 4.78 \times 10^{-9}$; (2) $C_\infty = 1.55 \times 10^{-8}$; (3) $C_\infty = 1.91 \times 10^{-8}$; (4) $C_\infty = 5.31 \times 10^{-8}$; and (5) $C_\infty = 1.78 \times 10^{-7}$. (c) The data in (b) normalized in terms of $\theta$ vs. $t'$: (1) $k = 0.39$, $\tau_D = 828$ s; (2) $k = 1.27$, $\tau_D = 82$ s; (3) $k = 1.56$, $\tau_D = 55$ s; (4) $k = 4.34$, $\tau_D = 7$ s; and (5) $k = 14.6$, $\tau_D = 0.6$ s.

manner and presented in Fig. 7a–c, respectively. Qualitatively, the same behavior is observed. For each concentration, the values for $\tau_D$ and $k$ are reported in the figure caption.

### 3.3. A surfactant with (apparent) repulsive interactions: $C_{12}E_8$

Finally, the surfactant $C_{12}E_8$ (octaethylene glycol mono-*n*-dodecyl ether) is discussed because positive $K$ values were required to describe the dynamic surface tension of this molecule. The equilibrium data are not reproduced here; the isotherm parameters reported in Table 1 were used to calculate $\tau_D$. The raw dynamic surface tension data are presented in Fig. 8a; the re-scaled data are presented in Fig. 8b. Again, the $\theta$ data nearly superpose. [If a simple Langmuir fit is used to define $\tau_D$, the data do not collapse as well (see Fig. 8c) but surface tension reductions still occur between 1 and 10 $\tau_D$ even using the cruder isotherm. This suggests that if only Langmuir parameters are available, even for repulsively interacting molecules, they still provide a useful means of normalizing data.]

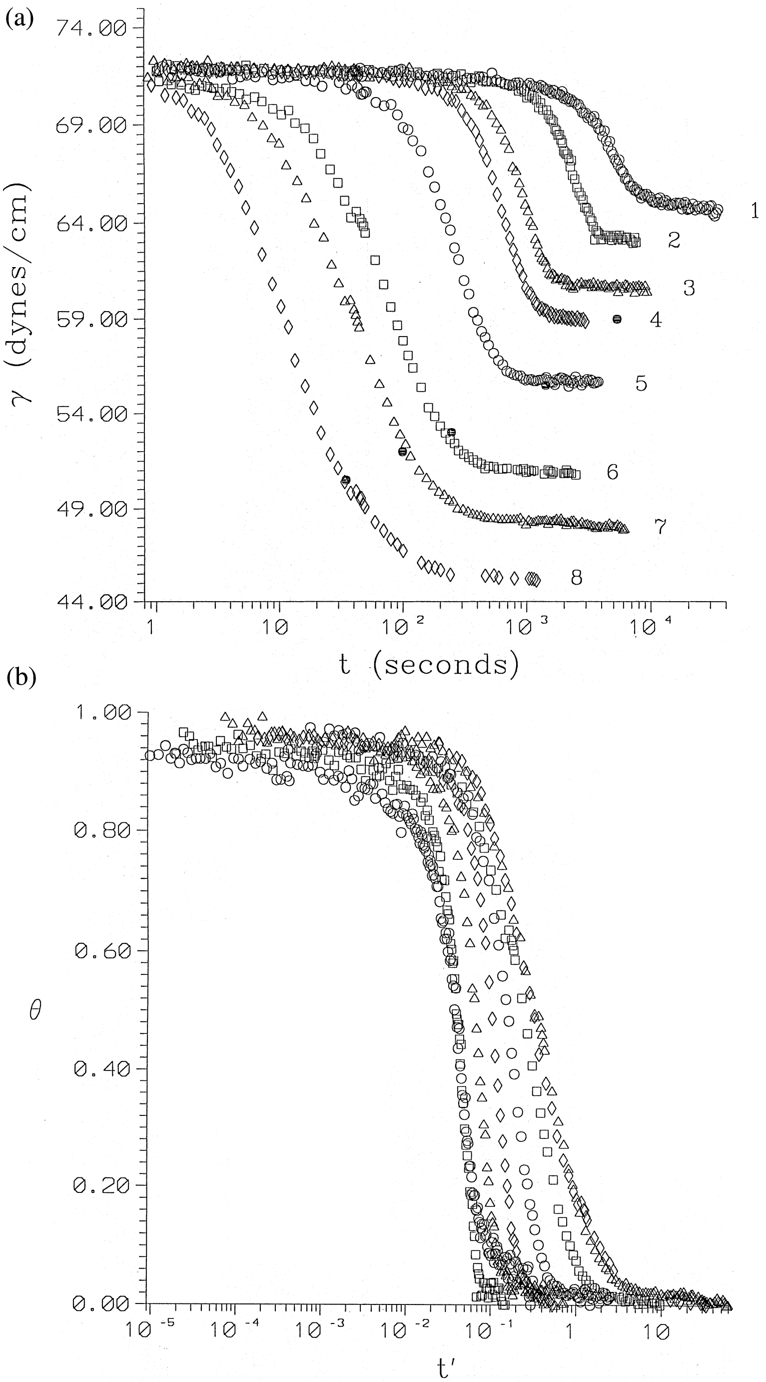
(a)
74.00
69.00
64.00
59.00
54.00
49.00
44.00
γ (dynes/cm)
1
10
10 ²
10 ³
10 ⁴
t (seconds)
1
2
3
4
5
6
7
8
(b)
1.00
0.80
0.60
0.40
0.20
0.00
θ
10 ⁻⁵
10 ⁻⁴
10 ⁻³
10 ⁻²
10 ⁻¹
1
10
t′

(c)

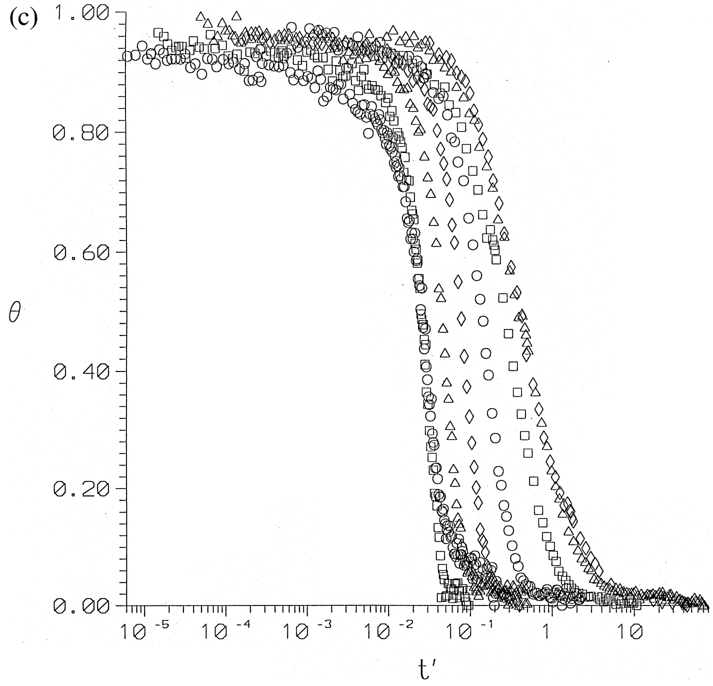

Fig. 8. (a) $\gamma$ (dyn/cm) vs. $t$ (s) for $C_{12}E_8$ for $C_\infty$ in mol/cm$^3$. The values for $k$ and $\tau_D$ based on the Frumkin isotherm are: (1) $C_\infty = 1.50 \times 10^{-10}$; (2) $C_\infty = 2.50 \times 10^{-10}$; (3) $C_\infty = 6.00 \times 10^{-10}$; (4) $C_\infty = 1.00 \times 10^{-9}$; (5) $C_\infty = 2.20 \times 10^{-9}$; (6) $C_\infty = 6.00 \times 10^{-9}$; (7) $C_\infty = 1.00 \times 10^{-8}$; and (8) $C_\infty = 1.50 \times 10^{-10}$. (b) The data in (a) normalized in terms of θ vs. $t'$ with the Frumkin-based diffusion time scale. The adsorption number and diffusion time scale are: (1) $k = 6$, $\tau_D = 1.12 \times 10^5$ s; (2) $k = 10$, $\tau_D = 5.18 \times 10^4$ s; (3) $k = 24$, $\tau_D = 1.30 \times 10^4$ s; (4) $k = 40.0$, $\tau_D = 5.65 \times 10^3$ s; (5) $k = 88$, $\tau_D = 1.50 \times 10^3$ s; (6) $k = 240$, $\tau_D = 260$ s; (7) $k = 400$, $\tau_D = 104$ s; and (8) $k = 713$, $\tau_D = 36.2$ s. (c) The data in (a) normalized in terms of θ vs. $t'$ with the Langmuir based adsorption number and diffusion time scale: (1) $k = 1.95$, $\tau_D = 1.69 \times 10^5$ s; (2) $k = 3.26$, $\tau_D = 8.14 \times 10^4$ s; (3) $k = 7.82$, $\tau_D = 1.90 \times 10^4$ s; (4) $k = 13.0$, $\tau_D = 7.5 \times 10^3$ s; (5) $k = 28.6$, $\tau_D = 1.68 \times 10^3$ s; (6) $k = 78.2$, $\tau_D = 235$ s; (7) $k = 130$, $\tau_D = 85.6$ s; and (8) $k = 232$, $\tau_D = 27.1$ s.

The Frumkin model with $K > 0$ describes the available data for the poly-ethoxylated surfactants well. (For example, it fits both the equilibrium $\gamma$ vs. $\ln C_\infty$ data and the $\gamma$ vs. $\Gamma$ data obtained by using the pendant bubble as a Langmuir trough for $C_{12}E_6$ [20]. This is described in Section 4.4.) However, the significance of $K > 0$ as indicating true intermolecular repulsion has been debated. An alternative adsorption isotherm and surface tension model has been proposed in which surfactant is assumed to adsorb and coexist in a number of states on the interface. The only poly-ethoxylated surfactant for which both Frumkin and the multi-state model have been fit is $C_{10}E_8$, which was studied by both Lin et al. using the Frumkin model (with three parameters obtained by regressing against the data) and Miller et al. [34] who assumed two coexisting surface states (with four parameters obtained from the equilibrium data.) Using the isotherm results published for $C_{10}E_8$ at a concentration of $10^{-8}$ mol/cm$^3$, and the diffusion coefficient estimated by the Wilke–Chang correlation [35], $\tau_D$ is 29 s for the two-state model, 41 s for the Frumkin model, in approximate agreement for a scaling argument.

## 4. Sorting surfactants using $\tau_D$: which surfactants reduce the surface tension faster?

Above, it was established that $\tau_D$ is a meaningful characteristic time scale by using it to scale several sets of dynamic surface tension data. In this section, $\tau_D$ is calculated and used to compare surfactants to predict which will reduce surface tension more rapidly. The sorting based on this scaling argument is then compared to the surface tension relaxation data obtained from the literature.

### *4.1. Comparing surfactants at fixed concentration*

The dynamic surface tension of five of these surfactants are compared at fixed bulk concentration $C_\infty$ of approximately $10^{-8}$ mol/cm$^3$. In the figure caption, the values for $\tau_D$ are given for each surfactant; the $k$ values are also reported using their best-fit isotherm. The raw surface tension relaxation profiles are reproduced in Fig. 9a for $C_{10}E_8$, Surfynol 104, $C_{12}E_6$, $C_{12}E_8$ and Triton-X 100; these data are recast in terms of $\theta$ vs. time (reported in seconds) in Fig. 9b. The surfactants reduce the surface tension in the order predicted by their $\tau_D$ values; $C_{10}E_8$ reduces surface tension fastest; Surfynol 104, $C_{12}E_6$ and $C_{12}E_8$ approximately superposing next, and Triton-X 100 last. All of these molecules have either weak interactions (Surfynol 104) or apparent repulsive interactions according to the best-fit Frumkin isotherm. For such molecules, the rate of surface tension reduction is predicted by $\tau_D$. (The Triton-X 100 data takes longer to equilibrate than is indicated by $\tau_D$. The authors of the Triton-X study attributed this to the fact that Triton-X 100 is a polydisperse surfactant. Miller at al. [36] showed that the long-time behavior of such surfactant mixtures is influenced by the presence of the surface active components present at low concentrations; these molecules require longer to diffuse to the interface, requiring more time to equilibrate.)

In Fig. 10a,b, three surfactants with strong attractive self-interactions are shown at concentrations of approximately $10^{-7}$ mol/cm$^3$: 1-octanol; 7-tetradecyn-6,9-diol and 1-decanol. For 1-octanol, $k \ll 1$ at this concentration. As predicted by the theoretical trace in Fig. 3b, the surface tension relaxation is skewed to times long compared to $\tau_D$. However, the remaining two traces are for $k > 1$; 7-tetradecyn-6,9-diol equilibrates faster than 1-decanol in agreement with the order predicted by $\tau_D$.

Finally, in Fig. 11a,b three poly-ethoxylated surfactants are compared at concentrations of approximately $10^{-9}$ mol/cm$^3$; $C_{10}E_8$, $C_{12}E_6$ and $C_{12}E_8$. For all three surfactants, $k > 1$, and the dynamic tensions reduce in the order predicted by $\tau_D$; $C_{10}E_8$, first, followed by $C_{12}E_6$, and $C_{12}E_8$, which nearly superpose. (For two of these curves, $h / a_B$ is greater than unity, i.e. for $C_{12}E_6$, $h / a_B = 1.3$; for $C_{12}E_8$,

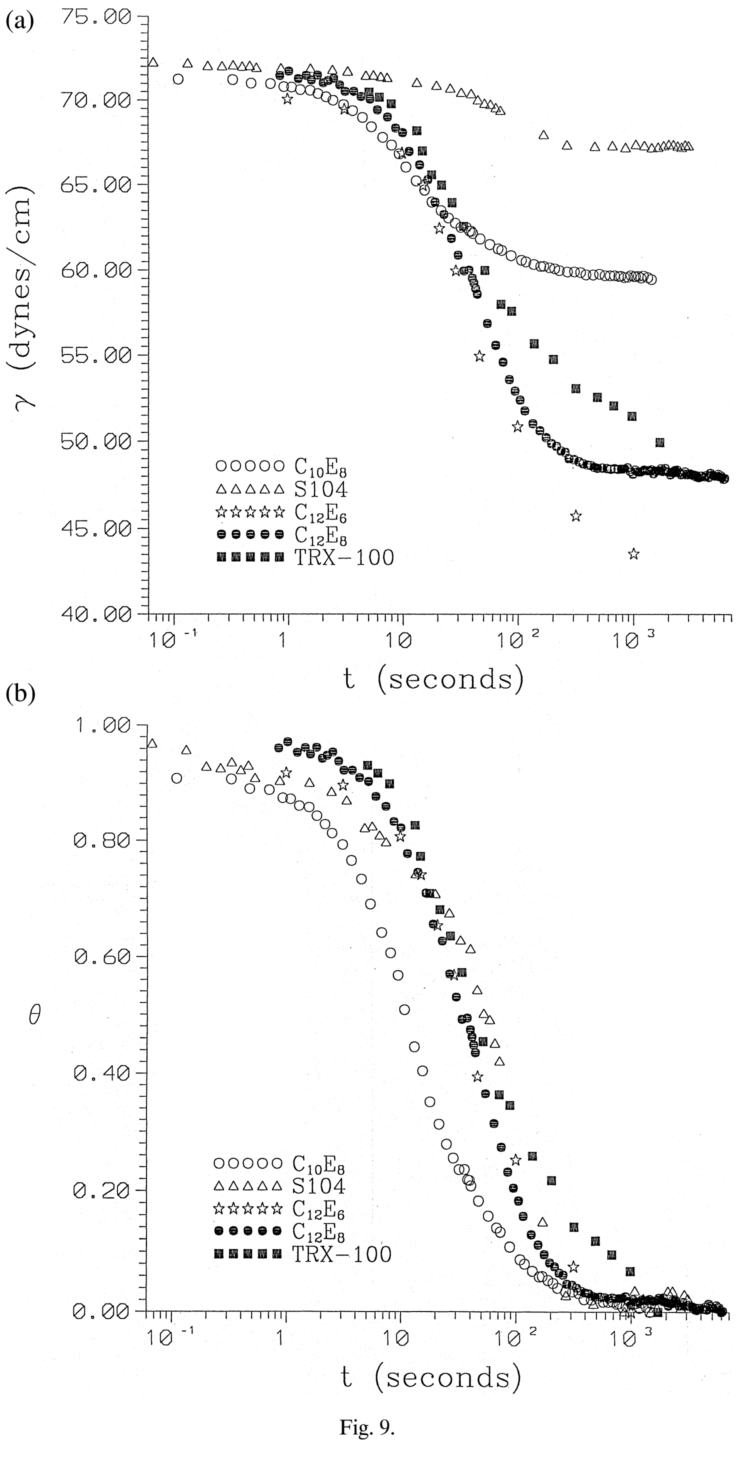
(a)
75.00
70.00
65.00
60.00
55.00
50.00
45.00
40.00
γ (dynes/cm)
10⁻¹
1
10
10²
10³
t (seconds)
○○○○○ C10E8
△△△△△ S104
☆☆☆☆☆ C12E6
●●●●● C12E8
■■■■■ TRX-100
(b)
1.00
0.80
0.60
0.40
0.20
0.00
θ
10⁻¹
1
10
10²
10³
t (seconds)
○○○○○ C10E8
△△△△△ S104
☆☆☆☆☆ C12E6
●●●●● C12E8
■■■■■ TRX-100

Fig. 9.

$h / a_B = 1.6$. These values are not large enough for curvature to strongly influence the system dynamics.)

### 4.2. Comparing surfactants at fixed equilibrium surface tension

A formulator often needs to understand which surfactant, for a given surface tension reduction, equilibrates the most rapidly. Such a comparison is shown in Fig. 12 for $\gamma_{eq}$ of approximately 50 dyn/cm. Once again, the raw surface tension data are given in Fig. 12a. The data are recast in terms of $\theta$ vs. time (in seconds) in Fig. 12b. The surface tension relaxations agree well with the ordering predicted by their $\tau_D$ values. Note that Surfynol-104 must be brought to very high bulk concentrations to reduce the tension, yielding a small $\tau_D$, and therefore a very rapid equilibration.

### 4.3. Convective effects

Many methods for characterizing surfactants involve leading order flow fields. For example, in the growing drop or maximum bubble pressure techniques, there is an influx of fluid at some prescribed flow rate into the drop or bubble. This flow field alters the surfactant mass transfer (see Levich [37]). However, diffusion from solution remains an important mechanism for surfactant delivery to the interface. If the rate of surface dilatation is fixed, the surfactant with the smallest value for $\tau_D$ should have the most rapid reduction in the surface tension.

### 4.4. The importance of obtaining equilibrium data

The variation in equilibration times from surfactant to surfactant is caused primarily by the variation in the adsorption depth $h$. This depth is calculated from the equilibrium isotherm which is fit to the equilibrium data. The quality of the estimate therefore depends on the quality of the equilibrium data on which it is based.

The most commonly used method for establishing a surface equation of state to relate $\gamma_{eq}$ to $\Gamma_{eq}$ is to measure $\gamma_{eq}$ as a function of $C_\infty$. A functional form for the adsorption isotherm relating $\Gamma_{eq}$ to $C_\infty$ is assumed. The corresponding function relating $\gamma_{eq}$ to $\Gamma_{eq}(C_\infty)$ is then regressed against the equilibrium data. This protocol was followed for most of the data discussed in this paper. The data were obtained using static methods such as the pendant bubble, pendant drop, or Wilhelmy plate techniques. Dynamic methods such as the maximum bubble pressure techniques

Fig. 9. (a) $\gamma$ (dyn/cm) vs. $t$ (s) for a variety of surfactants at an (approximately) fixed bulk concentration of approximately $10^{-8}$ mol/cm$^3$. $C_\infty$ reported in mol/cm$^3$: open circles: $C_{10}E_8$ at $C_\infty = 1.00 \times 10^{-8}$; open triangles: Surfynol 104 at $C_\infty = 0.66 \times 10^{-8}$; open stars: $C_{12}E_6$ at $C_\infty = 1.36 \times 10^{-8}$; filled circles: $C_{12}E_8$ at $C_\infty = 1.00 \times 10^{-8}$; and filled squares: Triton-X 100 at $C_\infty = 1.55 \times 10^{-8}$. (b) Normalized surface tension data from (a) reported in terms of $\theta$ vs. dimensional time: open circles: $k = 76.9$, $\tau_D = 47$ s; open triangles: $k = 1.32$, $\tau_D = 89$; open stars: $k = 390$, $\tau_D = 102$ s; filled circles: $k = 400$, $\tau_D = 104$ s; and filled squares: $k = 50$, $\tau_D = 117$ s.

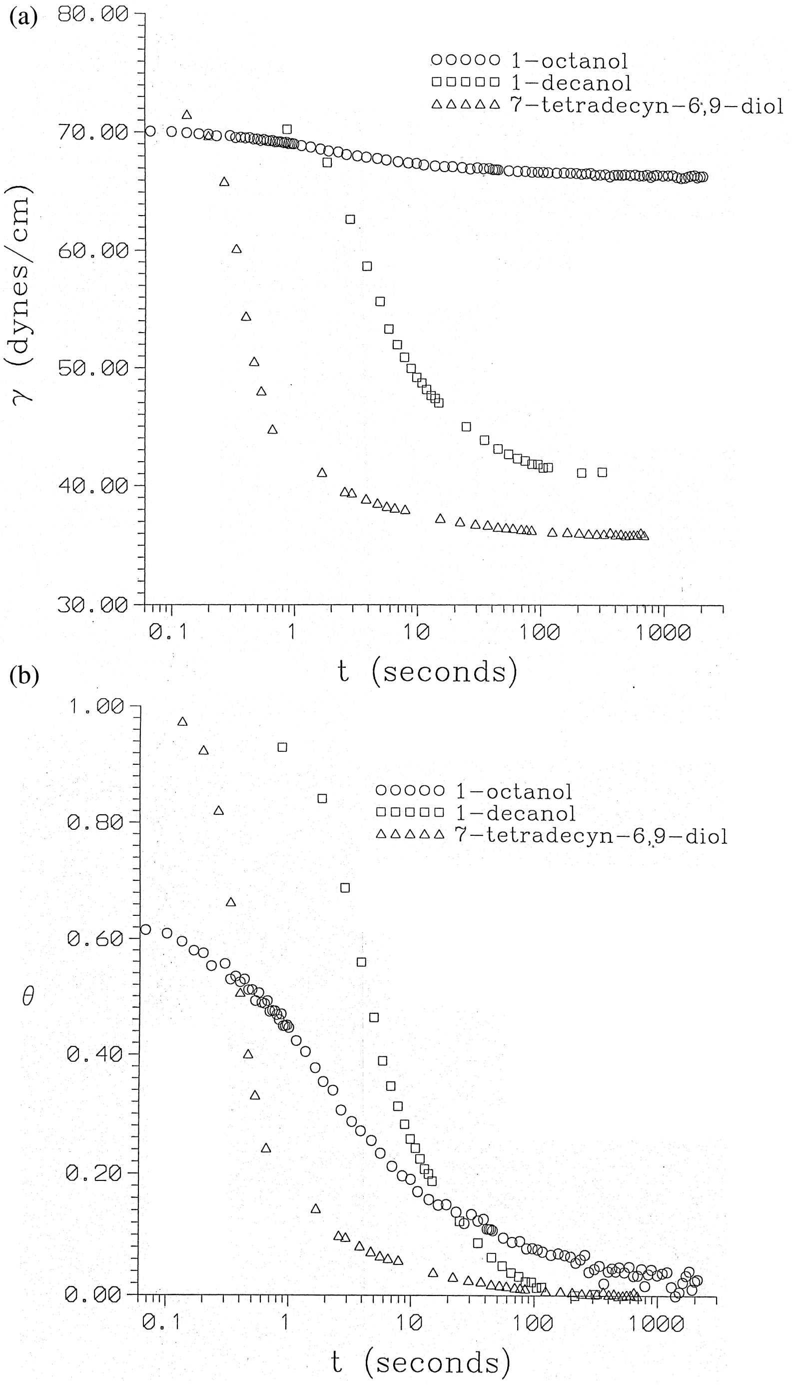
(a)
80.00
70.00
60.00
50.00
40.00
30.00
γ (dynes/cm)
○○○○○ 1-octanol
□□□□□ 1-decanol
△△△△△ 7-tetradecyn-6,9-diol
0.1
1
10
100
1000
t (seconds)
(b)
1.00
0.80
0.60
0.40
0.20
0.00
θ
○○○○○ 1-octanol
□□□□□ 1-decanol
△△△△△ 7-tetradecyn-6,9-diol
0.1
1
10
100
1000
t (seconds)

Fig. 10.

are inappropriate for this purpose, since the interface is continually deforming throughout the time that the measurement is made, and the rate of surface creation must be much slower than the diffusion rate to the interface in order to obtain an equilibrium measurement. For example, equilibrium surface tension data obtained by the pendant bubble and Wilhelmy plate techniques for Surfynol 104 are shown in Fig. 13a. The best-fit Langmuir isotherm is shown as the solid line. A family of curves in which the surface tension data vs. $C_\infty$ as a function of flow rate for the maximum bubble technique are also shown. Even at the slowest bubble formation rates the curves fail to superpose. Surfynol 104 has fast equilibration kinetics with the interface as shown in Fig. 5b. The discrepancy between the dynamic methods and the static methods is even worse for surfactants with larger $\tau_D$. This underscores the importance of using a static method to obtain equilibrium data.

Recently, Pan et al. [20] used a more direct method to relate the surface tension to the surface concentration. The needle from which the pendant bubble emerged in these experiments was attached to a syringe which allowed gas to be injected and withdrawn from the bubble. A pendant bubble was formed and allowed to equilibrate with a solution of $C_{12}E_6$ which had an equilibrium surface tension of 60 dyn/cm. The syringe pump was then programmed to rapidly expand and contract the bubble on time scales far more rapid than $\tau_D$ for this solution. The soluble surfactant adsorbed on the interface behaved as an insoluble monolayer under these conditions. Thus, the area change was inversely proportional to the surface concentration change. The figure is reproduced from their paper in Fig. 13b. The lack of hysteresis in the data indicate that the surface tension is in local equilibrium with the instantaneous surface concentration. These data allow a more direct comparison between experiment and the assumed form for the surface equation of state relating $\gamma_{\mathrm{eq}}$ to $\Gamma_{\mathrm{eq}}$. In particular, these data show the failure of the Langmuir model and adequate agreement of the Frumkin model with these data.

## 5. Guiding principles for comparing surfactants

### *5.1. Rapidly reducing surface tension to a low value*

Eq. (2) shows that for fixed $k = C_\infty/a$, the greater is $\Gamma_\infty$, the lower is the equilibrium surface tension. However, by increasing $\Gamma_\infty$, $\tau_D$ also increases. This can be offset by increasing the bulk concentration. The minimum value for $\tau_D$ occurs at the solubility limit or CMC, since the arguments behind the adsorption depth assume that $C_\infty$ is a monomeric bulk concentration. Typically, then, $k \gg 1$, and $\tau_D$

Fig. 10. (a) $\gamma$ (dyn/cm) vs. $t$ (s) for three surfactants with strong attractive self-interactions. $C_\infty$ reported in mol/cm$^3$: open circles: 1-octanol at $C_\infty = 2.00 \times 10^{-7}$; open squares: 1-decanol at $C_\infty = 2.09 \times 10^{-7}$; open triangles: 7-tetradecyn-6,9-diol at $C_\infty = 1.78 \times 10^{-7}$. (b) Normalized surface tension data from (a) reported in terms of $\theta$ vs. dimensional time. Open circles: $k = 0.36$, $\tau_D = 0.3$ s; open squares: $k = 2.3$, $\tau_D = 1.3$ s; open triangles: $k = 14.6$, $\tau_D = 0.6$ s.

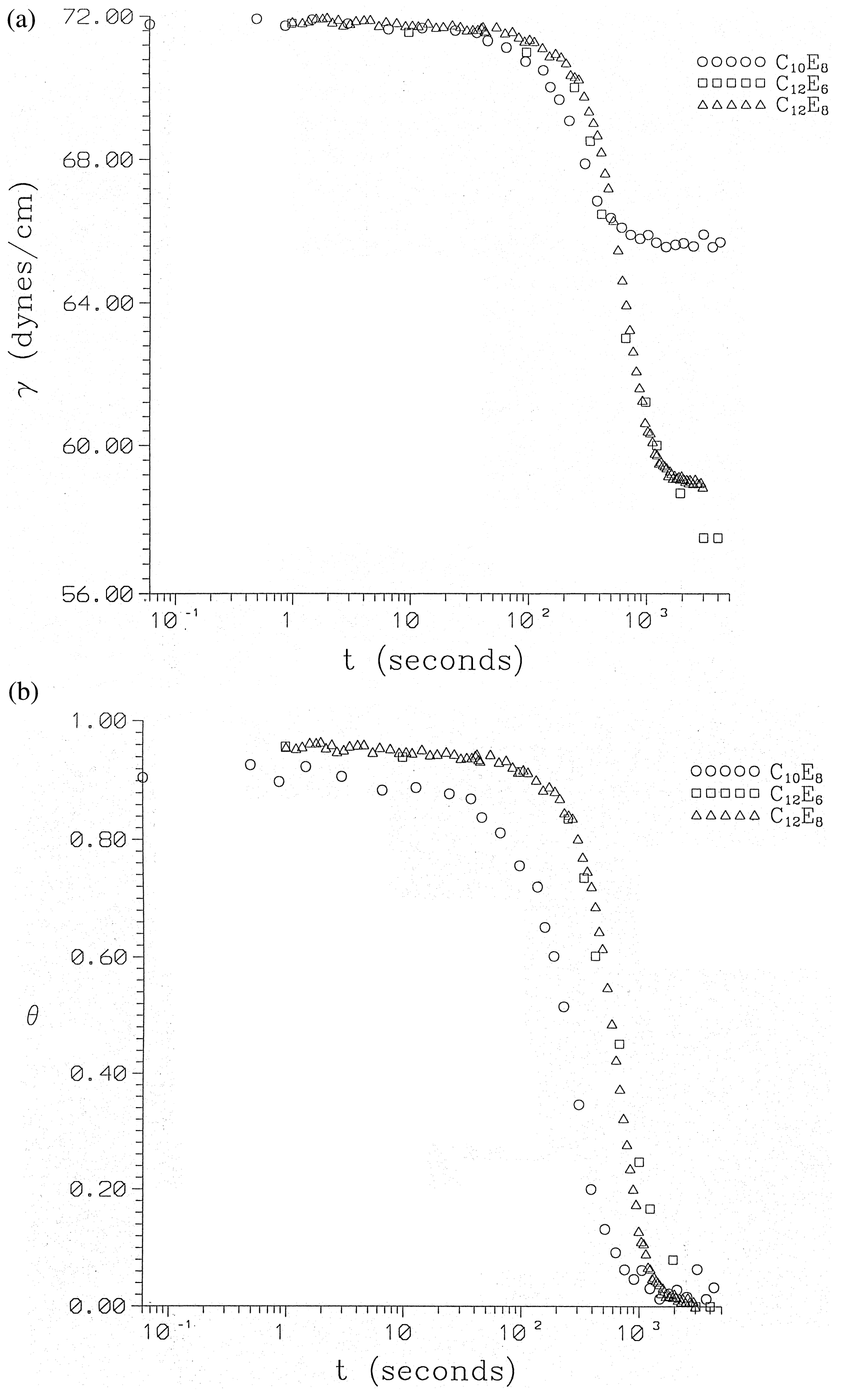
(a)
γ (dynes/cm)
72.00
68.00
64.00
60.00
56.00
10⁻¹
1
10
10²
10³
t (seconds)
○○○○○ C₁₀E₈
□□□□□ C₁₂E₆
△△△△△ C₁₂E₈
(b)
θ
1.00
0.80
0.60
0.40
0.20
0.00
10⁻¹
1
10
10²
10³
t (seconds)
○○○○○ C₁₀E₈
□□□□□ C₁₂E₆
△△△△△ C₁₂E₈

Fig. 11.

becomes:

$$\tau_{D_{\min}} = \frac{\Gamma_\infty^2}{D(\mathrm{CMC})^2} \tag{19}$$

Increases in $\tau_{D_{\min}}$ can be prevented if the CMC (or solubility limit) is increased proportionately to $\Gamma_\infty$. Thus, together, Eqs. (2) and (19) show the manner in which alterations in the surface activity, maximum packing and solubility interplay to determine both the time scale and the extent of surface tension reduction. These equations can be used to guide the engineering of surfactants for desired applications. (Note that Rosen's data [38] suggest that $\tau_D$ may be the relevant time scale applies to micellar systems. This is discussed further in Section 5.2.)

### *5.2. Discussion of guiding principles from structure–property studies*

From surfactant structure–property studies, a few guiding principles have been proposed relating to surface tension reduction. Many of the principles gleaned from these studies can be understood in terms of either $h$ or $\tau_D$.

In his text on surfactants, Rosen [39] proposes a manner of classifying the equilibrium behavior of surfactants in terms of two measures. He defines surfactant *efficiency* as the concentration required to reduce the surface tension by 20 dyn/cm, and surfactant *effectiveness* as the maximum reduction in surface tension attainable, either at the CMC or solubility limit. Rosen states that an efficient surfactant has a high value for the ratio $\Gamma_{eq}/(C_\infty d)$, which is simply $h/d$ in our nomenclature, where $d$ is the thickness of the interfacial region. Molecules with high efficiency therefore partition strongly to the interface at a low concentration. Neglecting variations in the thickness $d$ from surfactant to surfactant, the structure–property data for efficiency can be understood in terms of $h$, and the surface tension response in terms of the equation of state in Eq. (2). For example, Rosen reports that the surfactant efficiency (i.e. $h$) increases with carbon number in a linear chain surfactant. Indeed, since the surface activity of these molecules increases with carbon number (i.e. $1/a$ increases), and the area/molecule does not change strongly for a fixed headgroup (i.e. $\Gamma_\infty$ remains approximately constant) a lower bulk concentration is required to reach the $\Gamma_{eq}$ which reduces the surface tension by 20 dyn/cm. Thus, the required surface tension reduction occurs at a higher value for $h$. Rosen also notes that when linear chains are replaced by branched or unsaturated chains at fixed carbon number, the efficiency decreases. For this case, the limiting area molecule increases, or $\Gamma_\infty$ decreases. Since the surface tension reduces more weakly for molecules with smaller $\Gamma_\infty$, a higher bulk

---

Fig. 11. (a) $\gamma$ (dyn/cm) vs. $t$ (s) for three surfactants with repulsive self-interactions. $C_\infty$ reported in mol/cm$^3$: open circles: $C_{10}E_8$ at $C_\infty = 1.00 \times 10^{-9}$; open squares: $C_{12}E_8$ at $C_\infty = 1.00 \times 10^{-9}$; open triangles: $C_{12}E_6$ at $C_\infty = 1.36 \times 10^{-9}$. (b) Normalized surface tension data from (a) reported in terms of $\theta$ vs. dimensional time: open circles: $k = 7.70$, $\tau_D = 1960$ s; open squares: $k = 18.0$, $\tau_D = 5660$ s; open triangles: $k = 39.0$, $\tau_D = 5260$ s.

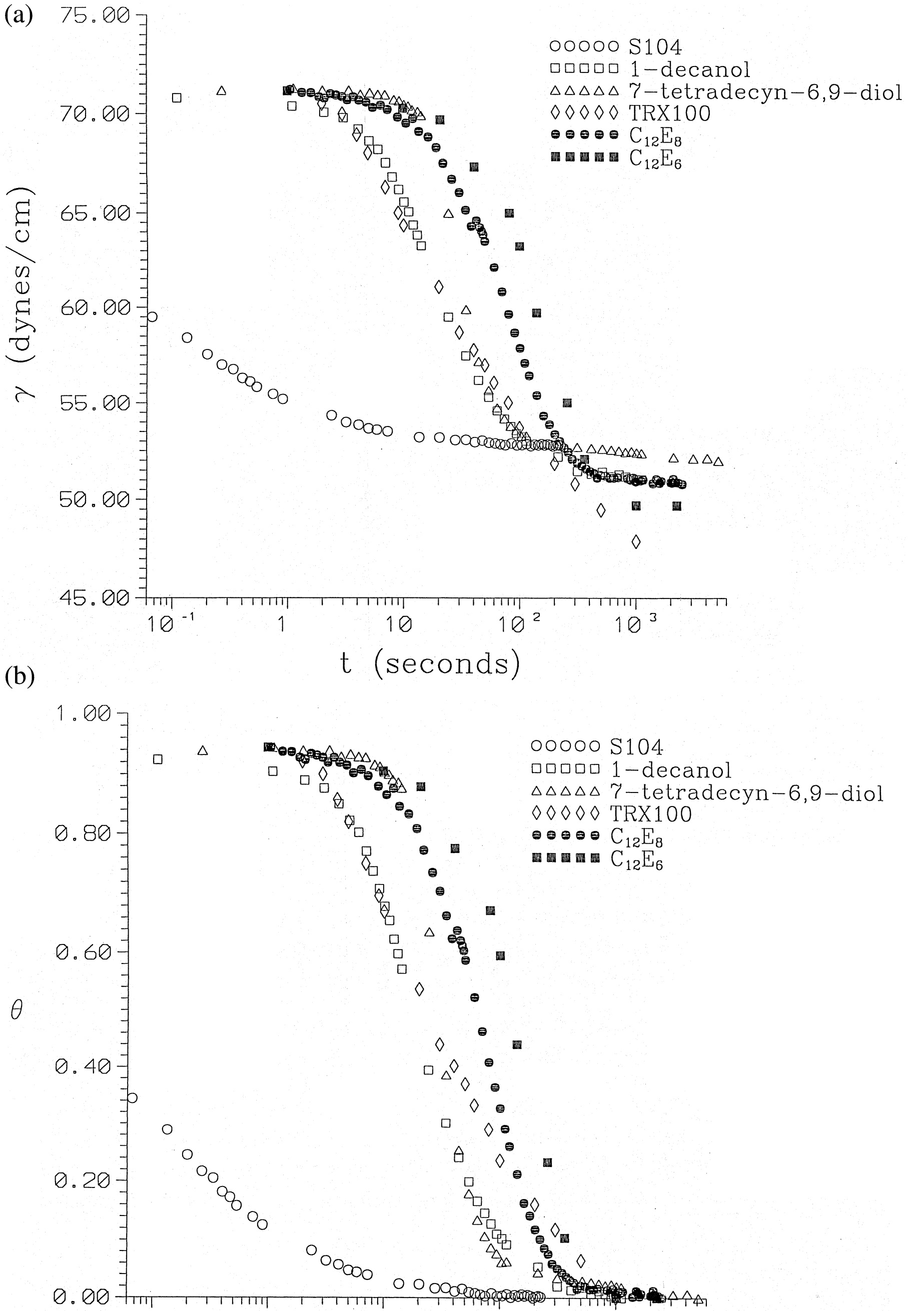
(a)
γ (dynes/cm)
75.00
70.00
65.00
60.00
55.00
50.00
45.00
t (seconds)
10⁻¹
1
10
10²
10³
○○○○○ S104
□□□□□ 1-decanol
△△△△△ 7-tetradecyn-6,9-diol
◊◊◊◊◊ TRX100
●●●●● C12E8
■■■■■ C12E6
(b)
θ
1.00
0.80
0.60
0.40
0.20
0.00
t (seconds)
10⁻¹
1
10
10²
10³
○○○○○ S104
□□□□□ 1-decanol
△△△△△ 7-tetradecyn-6,9-diol
◊◊◊◊◊ TRX100
●●●●● C12E8
■■■■■ C12E6

Fig. 12.

concentration is required to reduce the surface tension at fixed surface activity (i.e. higher $k$), so $h$ decreases.

While Rosen focused on the equilibrium efficiency of a surfactant, the analysis presented here suggests that molecules that are more efficient at low concentrations require longer times to equilibrate, since the diffusion time goes as the measure of the efficiency ($h$) squared. Suppose that several surfactants are compared at fixed bulk concentration; neglect the (typically small) variations in diffusivity $D$. If the tendency to adsorb ($1/a$) of the molecules differs strongly, but $\Gamma_\infty$ is comparable, the molecule with the smallest $a$ has the larger value for $h$. This molecule equilibrates slowest and reduces the surface tension to a lower equilibrium value. If the tendency to adsorb ($1/a$) of the molecules is comparable, but $\Gamma_\infty$ differs, the molecule with the largest $\Gamma_\infty$ will reduce the surface tension the most at equilibrium. It will also have the slowest rate. This is supported by the data of Rosen and Hua [40], who noted that in a given surfactant class (e.g. in a homologous series) compounds with larger $\Gamma_\infty$ require more time to reduce the surface tension.

There are other examples. In a study of the phosphine oxide surfactants by Wilhelmy plate and de Nouy ring techniques, Miller and Lunkenheimer [41] showed their adsorption dynamics to be well explained by diffusion-controlled adsorption. In the case of dodecyldimethyl phosphine oxide ($C_{12}$DMPO) the diffusion coefficient was reported to be $3 \times 10^{-6}$ cm$^2$/s and the Langmuir constants were reported in a later paper to be (Fang and Lunkenheimer [42]) $\Gamma_\infty = 4.26 \times 10^{-10}$ mol/cm$^2$; $a = 5.56 \times 10^{-9}$ mol/cm$^3$. An experiment for this molecule was performed at $C_\infty = 10^{-8}$ mol/cm$^3$, for which the equilibrium surface tension is approximately 63 dyn/cm. Using these data, $\tau_D$ can be calculated to be 246 s, in approximate agreement with the time required for the system to equilibrate. These authors note that 'since these surfactants are highly surface active, they form adsorption layers at low bulk concentrations, so that the time required to establish equilibrium adsorption is very long'. That is, since this molecule is efficient by Rosen's definition, it takes a prolonged time to equilibrate.

No such clear statement can be made about effective surfactants. If a surfactant is effective at reducing the surface tension because of an elevated CMC or solubility limit, $\tau_D$ will be small. If a surfactant is effective by having a large maximum packing, $\tau_D$ will be large. Therefore, a surfactant with greater effectiveness according to Rosen's criterion does not necessarily reduce the surface tension more rapidly.

Fig. 12. (a) $\gamma$ (dyn/cm) vs. $t$ (s) for a variety of surfactants at the bulk concentration of each required to give a surface tension reduction of ~ 20 dyn/cm. $C_\infty$ reported in mol/cm$^3$; $\gamma_{eq}$ reported in dyn/cm: open circles: Surfynol 104 at $C_\infty = 1.33 \times 10^{-7}$, $\gamma_{eq} = 52.75$; open squares: 1-decanol at $C_\infty = 5.24 \times 10^{-8}$, $\gamma_{eq} = 52.0$; open triangles: 7-tetradecyn-6,9-diol at $C_\infty = 1.91 \times 10^{-8}$, $\gamma_{eq} = 52.0$; open diamonds: Triton-X 100 at $C_\infty = 2.32 \times 10^{-8}$, $\gamma_{eq} = 47.5$; filled circles: $C_{12}E_8$ at $C_\infty = 6.00 \times 10^{-9}$, $\gamma_{eq} = 50.8$; filled squares: $C_{12}E_6$ at $C_\infty = 5.46 \times 10^{-9}$, $\gamma_{eq} = 49.5$. (b) Normalized surface tension data from (a) reported in terms of $\theta$ vs. dimensional time: open circles: $\tau_D = 0.6$ s; open squares: $\tau_D = 19$ s; open triangles: $\tau_D = 55$ s; open diamonds: $\tau_D = 57$ s; filled circles: $\tau_D = 260$ s; filled squares: $\tau_D = 506$ s.

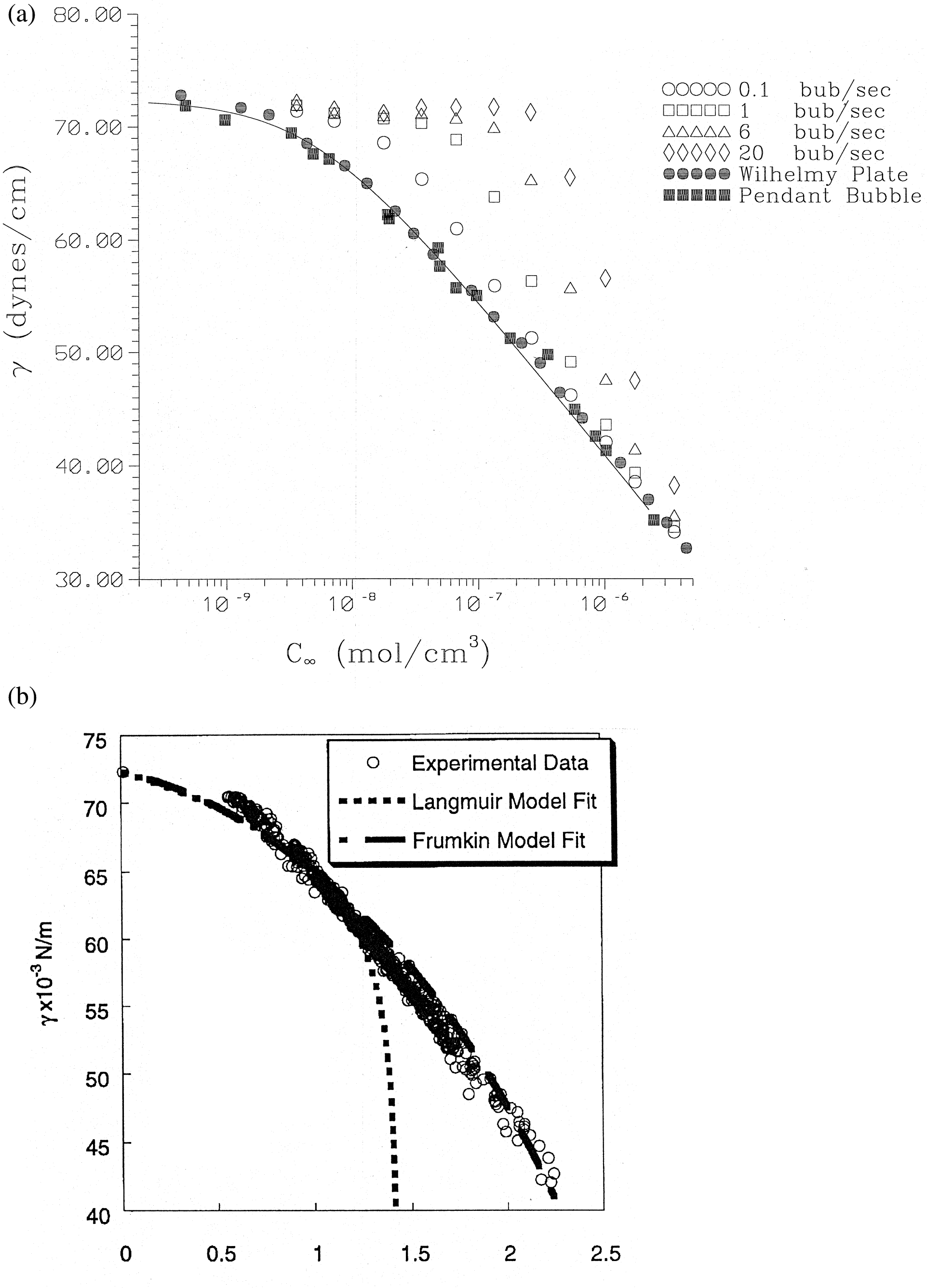
(a)
80.00
70.00
60.00
50.00
40.00
30.00
γ (dynes/cm)
$10^{-9}$
$10^{-8}$
$10^{-7}$
$10^{-6}$
$C_\infty$ (mol/cm$^3$)
○○○○○ 0.1 bub/sec
□□□□□ 1 bub/sec
△△△△△ 6 bub/sec
◊◊◊◊◊ 20 bub/sec
●●●●● Wilhelmy Plate
▨▨▨▨▨ Pendant Bubble
(b)
75
70
65
60
55
50
45
40
0
0.5
1
1.5
2
2.5
γx10$^{-3}$ N/m
Γ/Γ(γ=65 x10$^{-3}$ N/m)
○ Experimental Data
Langmuir Model Fit
Frumkin Model Fit

Fig. 13.

In a study using the maximum bubble pressure technique to study 15 highly purified surfactants, Rosen and Hua [40] proposed that 'surfactants that are more efficient at reducing the surface tension under equilibrium conditions are more efficient at reducing it in a short time'. This statement is in apparent contradiction with the discussion on surfactant efficiency above, in which the comparison of the dynamic and equilibrium behavior of surfactants was discussed at a given concentration. In Rosen and Hua, however, efficiency for the dynamic system is defined in terms of the bulk concentration required to reduce the surface tension by 20 dyn/cm *at a surface age of 1 s*. That is, dynamic efficiency was defined in terms of a much higher bulk concentration than was the equilibrium efficiency. The dynamic profiles in this work are consistent with the diffusion-controlled mechanisms discussed.

Note, there are surfactants which are *not* very surface active (so they must be present at high bulk concentration to reduce the equilibrium tension), but that equilibrate extremely rapidly. These surfactants have either high solubility limits or CMCs. Their high solubility allows their adsorption depths $h$, and therefore $\tau_D$ to be made small. As an example, the surface tension graphs of 2,7 dimethyl-4-octyn-3,6-diol taken from Ferri and Stebe [31] are shown in Fig. 14. These data were taken by pendant bubble technique. The equilibrium surface tension data, reported in Fig. 14a, were fitted to a Langmuir isotherm. The dynamic surface tension data are presented in Fig. 14b; $\tau_D$ values calculated from the Langmuir fit are reported in the figure caption. The surface tension evolution predicted by the diffusion-controlled model for this molecule is presented in Fig. 14c. It asymptotes to equilibrium at times earlier than the first pendant bubble image was obtained, confirming that these data are consistent with a diffusion-controlled mechanism. This surfactant is not efficient, but reduces the surface tension rapidly in a manner consistent with $\tau_D$.

The time scale $\tau_D$ or closely related parameters have been proposed or exploited in other dynamic surface tension studies. For example, the time scale $\tau_D$ has been used to recast Eq. (7) in dimensionless form by a number of authors (see, for example, [15,16,43]). The time scale was used by Lin et al. [15] to select a concentration range over which a surface tension relaxation would take long enough to study by the pendant bubble technique for Triton-X 100. The impor-

Fig. 13. (a) The surface tension as a function of bulk concentration for Surfynol 104. Equilibrium surface tension data were obtained by the pendant bubble technique and by the Wilhelmy plate. These data agree well with the best-fit Langmuir isotherm (solid curve). Surface tension data obtained by the maximum bubble pressure technique are larger than the equilibrium value. As the rate of bubble formation slows, the data approach the true equilibrium value. The maximum bubble pressure and Wilhelmy plate data were taken by Dr Greg Dado of Air Products and Chemicals, Inc. (b) The variation of the surface tension $\gamma$ as a function of the surface concentration $\Gamma$ for $C_{12}E_6$. These data were obtained by expanding and contracting a pendant bubble more rapidly than surfactant could diffuse to and from the interface. The adsorbed surfactant behaved as if it were insoluble during this experiment, allowing the relationship between $\gamma$ and $\Gamma$ to be directly explored with respect to a reference surface concentration. This figure is reproduced from the work of Pan et al. [19] in the *Journal of Colloid and Interface Science*.

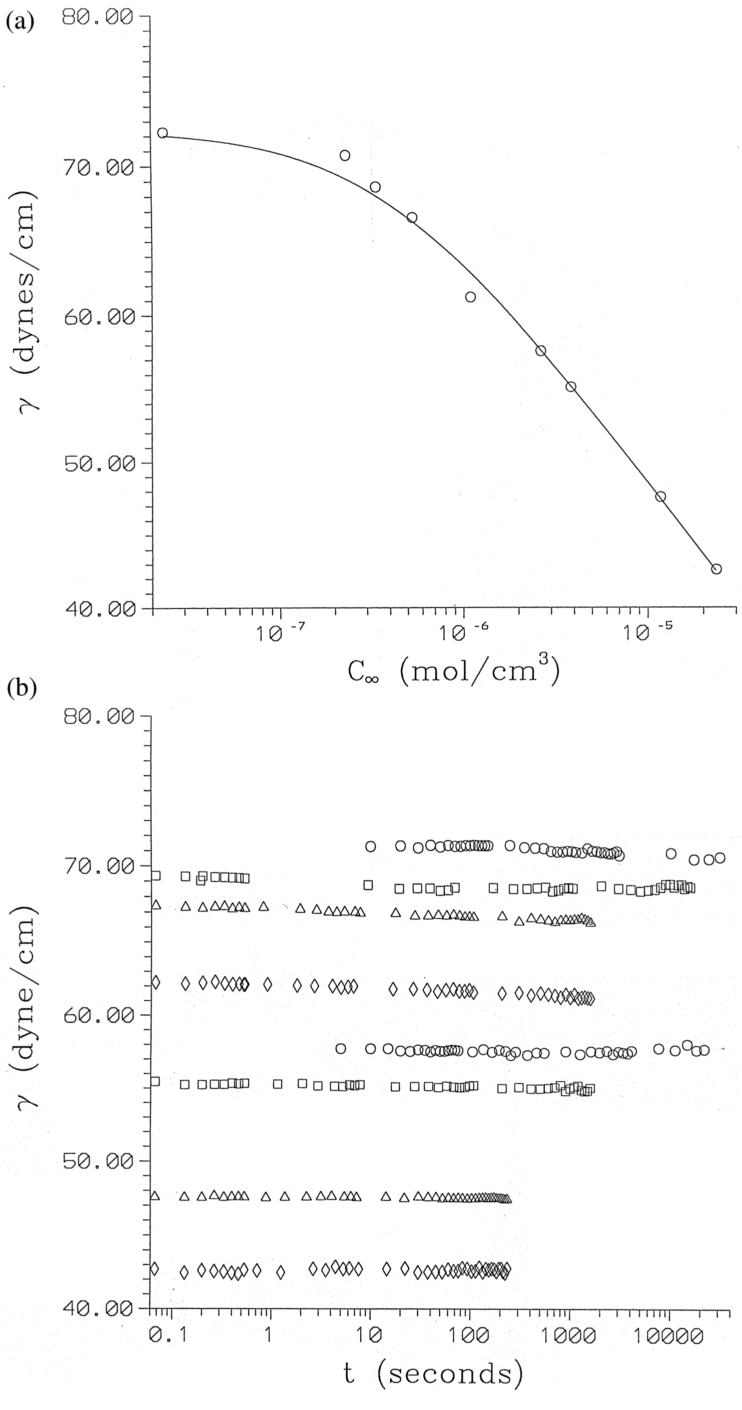
(a)
80.00
70.00
60.00
50.00
40.00
γ (dynes/cm)
10 -7
10 -6
10 -5
C∞ (mol/cm3)
(b)
80.00
70.00
60.00
50.00
40.00
γ (dyne/cm)
0.1
1
10
100
1000
10000
t (seconds)

(c)

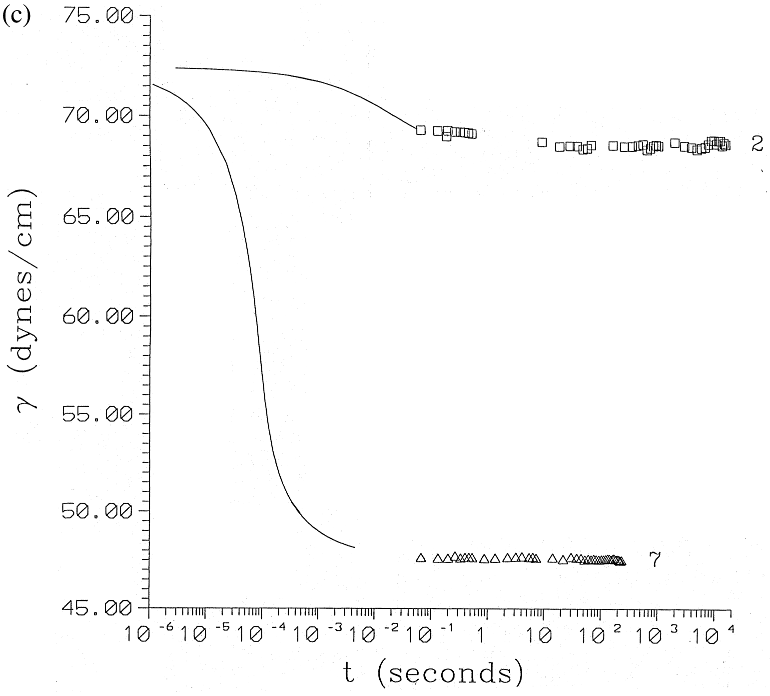

Fig. 14. The equilibrium surface tension vs. bulk concentration for 2,4-dimethyl–4-octyn-3,6-diol [$\gamma_{eq}$ (dyn/cm) vs. $C_\infty$]. The solid line is the best fit to the Langmuir model. The isotherm parameters are given in Table 1. (b) γ (dyn/cm) vs. $t$ (s) for 2,4-dimethyl–4-octyn-3,6-diol for $C_\infty$ in mol/cm$^3$: (1) $C_\infty = 2.34 \times 10^{-7}$, $k = 0.554$, $\tau_D = 0.04$ s; (2) $C_\infty = 3.41 \times 10^{-7}$, $k = 0.81$, $\tau_D = 0.03$ s; (3) $C_\infty = 5.38 \times 10^{-7}$, $k = 1.28$, $\tau_D = 0.02$ s; and (4) $C_\infty = 1.11 \times 10^{-6}$, $k = 2.63$, $\tau_D = 0.007$s; (5) $C_\infty = 2.68 \times 10^{-6}$, $k = 6.35$, $\tau_D = 0.001$ s, (6) $C_\infty = 3.90 \times 10^{-6}$, $k = 9.24$, $\tau_D = 0.0009$ s; (7) $C_\infty = 1.18 \times 10^{-5}$, $k = 28.0$, $\tau_D = 0.001$ s; and (8) $C_\infty = 2.35 \times 10^{-5}$, $k = 55.7$, $\tau_D = 0.00003$ s. (c) Curves 2 and 7 are reproduced from Fig. 14b. For the square symbols (labeled curve 2) $C_\infty = 3.41 \times 10^{-7}$ mol/cm$^3$; for the circular symbols (labeled curve 7) $C_\infty = 1.18 \times 10^{-5}$ mol/cm$^3$. The first data point for these curves is obtained within approximately 0.06 s of bubble formation. The surface tension has equilibrated within this time. This is consistent with a diffusion controlled adsorption model (solid curves) for this surfactant at both concentrations, obtained using Langmuir parameters and the diffusion coefficient obtained by PFGSE-NMR.

tance of $\tau_D$ in sorting surfactants has appeared in studies by Hua and Rosen [38–40,44], who note that the time scale $t^*$ for surface tension reduction in the maximum bubble pressure technique reduces with increased bulk concentration. They estimate $t^*$ by using the forward diffusion term in the Ward and Tordai expression [i.e. $\Gamma \sim 2C_\infty(Dt/\pi)^{1/2}$], estimating Γ by $\Gamma_\infty$ and $t$ by $t^*$. Solving for $t^*$:

$$t^* = \frac{\pi}{4}\frac{\Gamma_\infty^2}{C_\infty^2}\frac{1}{D} \tag{20}$$

and approximating $\pi/4$ as unity and solving for $t^*$, it is clear that $t^*$ is simply $\tau_D$. By measuring the time for the surface tension to reach a plateau is the maximum bubble pressure studies, the slope of $\log t^*$ was calculated as a function of $\log \Gamma_\infty/C_\infty$, slopes ranging from 1.3 to 2.2 were found, in approximate agreement with the theoretical prediction of 2.0 for this slope. Maximum bubble pressure data for *n*-dodecyl-benzyl-*n*-methyl-glycine [38] taken by Hua and Rosen show that proportionality between $t^*$ and the inverse square bulk concentration persists even above the CMC. This suggests that $\tau_D$ is the relevant time scale for diffusion to the interface for micellar solutions if the rate of demicellization is rapid.

Finally, in recent studies designed to measure surfactant adsorption–desorption dynamics, the change in $\tau_D$ with bulk concentration is exploited, as described below.

## 6. Finite adsorption–desorption kinetics

In recent studies of surfactant mass transfer, the concept of a shift in controlling mechanism from diffusion control at low concentrations to adsorption–desorption control at high concentrations was developed [20,21,43] and used to design experiments to measure these kinetic constants [20,21,23].

To motivate the concept of a shift of mechanism, Pan et al. [20] consider a surfactant which obeys a Langmuir model in the kinetically controlled limit. In this case, $C_s = C_\infty$ and $\Gamma$ is determined by:

$$\frac{\partial \Gamma}{\partial t} = \beta C_\infty(\Gamma_\infty - \Gamma) - \alpha\Gamma \tag{21a}$$

where $\alpha$ and $\beta$ are the kinetic constants for desorption and adsorption, respectively; the ratio $\alpha/\beta$ is the adsorption parameter $a$. The solution for $\Gamma(t)$ in this limit is:

$$\Gamma = \Gamma_{\mathrm{eq}}[1 - \exp(-\alpha(1+k)t)] \tag{21b}$$

so $1/[\alpha(1+k)]$ is the characteristic time scale for adsorption–desorption. Therefore, the ratio of diffusion to adsorption–desorption time scales is:

$$\frac{\tau_D}{\tau_{kin}} = \frac{\Gamma_\infty^2\alpha}{a^2(1+k)} \tag{22}$$

Since $k$ is a scaled concentration, the time scale for diffusion reduces compared to that for adsorption–desorption. If this ratio becomes small enough, then adsorption–desorption kinetics can play a strong role in determining the time required for the system to equilibrate. In this case, the arguments developed in this paper for predicting surfactant dynamics would have to be augmented by comparing the kinetic constants for adsorption–desorption for the surfactants.

The magnitudes of the adsorption–desorption kinetic constants are still being established experimentally. Values have been obtained by using the concept of shift of mechanism to study surface tension evolutions obtained in by adsorption to a freshly formed pendant bubble in solution. Another technique has been used, which also uses a pendant bubble [45]. A pendant bubble is formed in surfactant solution, equilibrated, and subsequently compressed to pack surfactant above its equilibrium adsorption. In order to equilibrate, surfactant must desorb from the surfactant-laden interface. In these studies, pendant bubble images are obtained to study the subsequent increase of the surface tension as surfactant desorbs and diffuses away to restore equilibrium. These profiles require mixed kinetic-diffusion models to explain the surface tension evolution.

Any kinetic barrier which exerts a controlling influence on the mass transfer, would require longer times to equilibrate than a diffusion controlled process. Even under these circumstances, however, $\tau_D$ is a useful lower bound for the equilibration time, since mass transfer cannot be faster than the predicted diffusion-controlled evolution.

## 7. Conclusions

A diffusion time scale $\tau_D$ was described as the relevant scaling for diffusion-controlled adsorption to a planar interface. By integrating the Ward and Tordai equations for molecules with and without nearest neighbor interactions, the surface tension for diffusion controlled surfactants was shown to equilibrate within 1–10 $\tau_D$. The time scale, when used to renormalize dynamic surface tension data was shown to allow high concentration ($k \gg 1$) surface tension data nearly to superpose. The utility of $\tau_D$ in sorting surfactants in terms of their ability to reduce surface tension rapidly was demonstrated on a variety of dynamic surface tension data sets. Finally, guiding principles that have been proposed in the literature in structure–property studies were shown to be consistent with the trends predicted by $\tau_D$.

Since $\tau_D = h^2/D$, and $h$ is determined by isotherm parameters, this work underscores the importance of understanding the equilibrium behavior of surfactant solutions in order to understand their dynamics. Finally, even for surfactants with mixed kinetic-diffusion control, $\tau_D$ represents the fastest characteristic time for the interface to equilibrate.

## Nomenclature

| | |
|---|---|
| $a$: | the tendency of molecules to adsorb on the interface |
| $a_B$: | the radius of a pendant bubble |
| $\mathrm{d}A$: | a differential area element |
| $h$: | the adsorption depth defined in Eq. (4) |

$k$: the adsorption number defined in Eq. (12)

$x$: the fractional coverage of surfactant on the interface in equilibrium with $C_\infty$

*CMC:* critical micelle concentration

$C_\infty$: the bulk concentration of surfactant in solution

$C_s$: the concentration in the sublayer immediately adjacent to the interface

$C'_s$: a dimensionless sublayer concentration; defined in Eq. (8)

$D$: the diffusivity of surfactant in solution

$F$: Faraday's constant

$K$: the interaction parameter in a Frumkin model; $K > 0$ for repulsion, $K < 0$ for cohesion.

$RT$: the product of the ideal gas constant and the temperature

$t$: time

$t'$: the dimensionless time, defined in Eq. (8)

$z$: the surfactant valence, used in Eqs. (16a), (16b), (16c), (17a) and (17b)

$\alpha$: the desorption kinetic constant

$\beta$: the adsorption kinetic constant

$\gamma_{\text{eq}}$: the equilibrium surface tension, defined in Eq. (2) for surfactants obeying a Langmuir model

$\gamma_o$: the surface tension of the surfactant-free interface

$\gamma(\Gamma)$: the surface tension in equilibrium with $\Gamma$

$\epsilon$: the permittivity of the surfactant solution used in Eqs. (17a) and (17b)

$\kappa$: the inverse Debye length defined in Eq. (16c)

$\theta$: the dimensionless surface tension reduction defined in Eq. (8)

$\Gamma(t)$: the surface concentration of surfactant and any instant in time

$\Gamma'$: the dimensionless surface concentration of surfactant, defined in Eq. (8)

$\Gamma_\infty$: the maximum packing on the interface, or the inverse minimum area/molecule

$\tau_D$: the diffusion time scale, defined in Eq. (3)

$\Psi_s$: the surface potential

## References

[1] M. Rosen, Surfactants and Interfacial Phenomena, John Wiley and Sons, New York, 1978.

[2] A. Adamson, A. Gast, Physical Chemistry of Surfaces, 6th ed., John Wiley and Sons, New York, 1997.

[3] D.H. Smith (Ed.), Surfactant Based Mobility Control, A.C.S. Symposium Series 373 (1988).

[4] T.h.F. Tadros, Surfactants in Agrochemicals, Surfactant Science Series 54, Marcel Dekker, New York, 1995.

[5] M. El-Nokay, D. Cornell (Eds.), Microemulsions and Emulsions in Foods, A.C.S. Symposium Series 448 (1991).

[6] M.M. Reiger, L.D. Rhein, Surfactants in Cosmetics, Surfactant Science Series 68, Marcel Dekker, New York, 1997.

[7] F.M. Fowkes, J. Phys. Chem. 57 (1983) 98.

[8] M.J. Rosen, X.Y. Hua, J. Colloid Interface Sci 139 (1990) 397.

[9] C.H. Chang, E.I. Franses, Colloids Surf. A 100 (1995) 1.

[10] R. Miller, P. Joos, V. Fainerman, Adv. Colloid Interface Sci. 49 (1994) 249.
[11] A. Frumkin, Z. Phys. Chem. 116 (1925) 466.
[12] J.T. Davies, Proc. R. Soc. A. London 245 (1958) 417,429.
[13] A.F.H. Ward, L. Tordai, J. Chem. Phys. 14 (1946) 453.
[14] R. Miller, G. Kretchmar, Colloid Polym. Sci. 258 (1980) 85.
[15] S.Y. Lin, K. McKeigue, C. Maldarelli, AIChE J. 36 (1990) 1785.
[16] S.Y. Lin, K. McKeigue, C. Maldarelli, Langmuir 7 (1991) 1055.
[17] S.Y. Lin, K. McKeigue, C. Maldarelli, Langmuir 10 (1994) 3442.
[18] S.Y. Lin, W.B. Hwang, T.L. Lu, Colloids Surf. A 114 (1996) 143.
[19] C.T. Hsu, C.H. Chang, S.Y. Lin, Langmuir [submitted].
[20] R. Pan, J. Green, C. Maldarelli, J. Colloid Interface Sci. 205 (1998) 213.
[21] R. Pan, C. Maldarelli, B. Ennis, J. Green, in: V. Pillai, D.O. Shah (Eds.), Dynamic Properties of Interfaces and Associated Structures, AOCS Press, 1996, pp. 23–47.
[22] S.Y. Lin, T.L. Lu, W.B. Hwang, Langmuir 11 (1995) 555.
[23] D.O. Johnson, K.J. Stebe, J. Colloid Interface Sci. 182 (1996) 179.
[24] J.K. Ferri, K.J. Stebe, J. Colloid Interface Sci. 209 (1999) 1.
[25] C.H. Chang, E. Franses, Chem. Eng. Sci. 49 (1994) 313.
[26] C.A. MacLeod, C.J. Radke, Langmuir 10 (1994) 3555.
[27] S.S. Datwani, K.J. Stebe, J. Colloid Interface Sci. [in review].
[28] V.B. Fainerman, Colloid J. USSR 40 (1978) 769.
[29] H.C. Chang, C.T. Hsu, S.Y. Lin, Langmuir 14 (1998) 2476.
[30] S.Y. Lin, R.Y. Tsay, L.W. Lin, S.I. Chen, Langmuir 12 (1996) 6530.
[31] J.K. Ferri, K.J. Stebe, Colloids Surf. A [in press].
[32] S.Y. Lin, W.J. Wang, C.T. Hsu, Langmuir 13 (1997) 6211.
[33] P. Stilbs, Prog. NMR Spectrosc. 19 (1987) 1.
[34] R. Miller, E.V. Aksenenko, L. Liggieri, F.J. Ravera, M. Ferrari, V.B. Fainerman, Langmuir 15 (1999) 1328.
[35] C.R. Wilke, P. Chang, AIChE J. 1 (1955) 264.
[36] R. Miller, K. Lunkenheimer, G. Kretschmar, Colloid Polym. Sci. 257 (1979) 1118.
[37] B.G. Levich, Physicochemical Hydrodynamics, Prentice Hall, New Jersey, 1967.
[38] X.Y. Hua, M.J. Rosen, J. Colloid Interface Sci. 124 (1988) 652.
[39] M.J. Rosen, Surfactants and Interfacial Phenomena, John Wiley and Sons, Inc, New York, 1978.
[40] M.J. Rosen, X.Y. Hua, J. Colloid Interface Sci. 139 (1990) 397.
[41] R. Miller, K. Lunkenheimer, Colloid Polym. Sci. 264 (1986) 357.
[42] J.P. Fang, K. Lunkenheimer, J. Phys. Chem. A 99 (1995) 4632.
[43] S.Y. Lin, H.C. Chang, E.M. Chen, J. Chem. Eng. Jpn. 29 (1996) 634.
[44] X.Y. Hua, M.J. Rosen, J. Colloid Interface Sci. 141 (1991) 180.
[45] S.Y. Lin, L.W. Lin, S.I. Chen, Langmuir 13 (1997) 3191.